UNCLASSIFIED

AD 463855

DEFENSE DOCUMENTATION CENTER

FOR

SCIENTIFIC AND TECHNICAL INFORMATION

CAMERON STATION ALEXANDRIA, VIRGINIA

UNCLASSIFIED

NOTICE: When government or other drawings, specifications or other data are used for any purpose other than in connection with a definitely related government procurement operation, the U. S. Government thereby incurs no responsibility, nor any obligation whatsoever; and the fact that the Government may have formulated, furnished, or in any way supplied the said drawings, specifications, or other data is not to be regarded by implication or otherwise as in any manner licensing the holder or any other person or corporation, or conveying any rights or permission to manufacture, use or sell any patented invention that may in any way be related thereto.

463855

CATALOGED BY: DDC
AS AD No. 463855

AVAILABLE COPY WILL NOT PERMIT
FULLY LEGIBLE REPRODUCTION.
REPRODUCTION WILL BE MADE IF
REQUESTED BY USERS OF DDC.

Alkaline Battery Division

GULTON INDUSTRIES, INC.

Metuchen, N. J.

BEST
AVAILABLE COPY

AVAILABLE COPY WILL NOT PERMIT
FULLY LEGIBLE REPRODUCTION.
REPRODUCTIONS WILL BE MADE IF
REQUESTED BY USERS OF DDC.

THIRD QUARTERLY TECHNICAL PROGRESS REPORT ON INVESTIGATION OF HERMETICALLY SEALED MAINTENANCE-FREE, HIGH RATE, NICKEL-CADMIUM BATTERIES FOR AIRCRAFT APPLICATIONS

MAY, 1965

DDC
RECEIVED
JUN 1 1965
DDC-IRA E

AIR FORCE AERO PROPULSION LABORATORY
RESEARCH AND TECHNOLOGY DIVISION
AIR FORCE SYSTEMS COMMAND, USAF
WRIGHT-PATTERSON AIR FORCE BASE, OHIO. 45433

PROJECT NO. 8173
TASK NO. 817304

PREPARED UNDER CONTRACT NO. AF 33(615)-2087
BY GULTON INDUSTRIES, INC.
ALKALINE BATTERY DIVISION
METUCHEN, NEW JERSEY

AUTHORS: E. KANTNER, R. V. TARANTINO, H. M. SEIGER
AND R. C. SHAIR

NOTICES

Foreign announcement and distribution of this report is not authorized.

The distribution of this report is limited because it contains technology identifiable with items on the strategic embargo list excluded from export or re-export under U. S. Export Control Act of 1949 (63 STAT. 7), as amended (50 USC App. 2020.2031), as implemented by AFR 400-10.

The work covered by this report was accomplished under Air Force Contract AF33(615)-2087, but this report is being published and distributed prior to Air Force review. The publication of this report, therefore, does not constitute approval by the Air Force of the findings or conclusions contained herein. It is published for the exchange and stimulation of ideas.

TABLE OF CONTENTS

		PAGE NO.
I.	ABSTRACT	1
II.	INTRODUCTION	3
III.	BATTERY RESEARCH & DEVELOPMENT	4
	A. EFFECT OF PLATE THICKNESS ON SEALED CELL BEHAVIOR DURING HIGH RATES OF CHARGE & DISCHARGE	4
	B. EFFECT OF IMPURITIES ON SELF-DISCHARGE OF SEALED NICKEL-CADMIUM CELLS	7
	C. EFFECT OF RUBIDIUM AND CESIUM ON SEALED CELL BEHAVIOR AT HIGH RATES OF DISCHARGE	10
IV.	BATTERY CHARGE CONTROL	15
	A. COULOMETER CHARGE CONTROL	15
	B. CHARGE CONTROL CIRCUIT	16
V.	CONCLUSIONS	19

LIST OF TABLES

		PAGE NO.
I	AH CAPACITIES OF SEALED CELLS WITH VARYING PLATE THICKNESS AT 0°F	5
II	WEIGHT GAINS OF SINTERED NICKEL PLAQUES	7
III	AH CAPACITIES OF HIGH PURITY CELLS	10
IV	WEIGHT GAINS OF BATTERY PLATES	11
V	CHARGE AND DISCHARGE RATES, AND AH CAPACITIES OF FORMATION CELLS	11
VI	AH CAPACITIES OF CELL CONTAINING ELECTROLYTE ADDITIVES	13
VII	AH CAPACITIES OF CELLS AT 60 AMPERE DISCHARGE RATE	13

LIST OF FIGURES

FIGURE NO.	
1.	VOLTAGE VS. TIME 5 AMPERE DISCHARGE AT 0°F
2.	VOLTAGE VS. TIME 10 AMPERE DISCHARGE AT 0°F
3.	VOLTAGE VS. TIME 15 AMPERE DISCHARGE AT 0°F
4.	VOLTAGE VS. TIME 20 AMPERE DISCHARGE AT 0°F
5.	VOLTAGE VS. TIME 25 AMPERE DISCHARGE AT 0°F
6.	VOLTAGE VS. TIME 30 AMPERE DISCHARGE AT 0°F
7.	VOLTAGE VS. TIME 40 AMPERE DISCHARGE AT 0°F
8.	VOLTAGE VS. TIME 50 AMPERE DISCHARGE AT 0°F
9.	VOLTAGE VS. TIME 60 AMPERE DISCHARGE AT 0°F
10.	VOLTAGE VS. TIME 60 AMPERE DISCHARGE AT ROOM TEMP.
11.	VOLTAGE VS. TIME 60 AMPERE DISCHARGE AT ROOM TEMP.
12.	VOLTAGE VS. TIME 60 AMPERE DISCHARGE AT ROOM TEMP.
13.	EFFECT OF RUBIDIUM AND CESIUM ON CELL VOLTAGE AND CAPACITY AT HIGH DISCHARGE RATE
14.	COULOMETER VOLTAGE VS. TIME 10 AMPERE DISCHARGE AT ROOM TEMP.
15.	COULOMETER VOLTAGE VS. TIME 100 AMPERE DISCHARGE AT ROOM TEMP.
16.	COULOMETER VOLTAGE VS. TIME 200 AMPERE DISCHARGE AT ROOM TEMP.
17.	COULOMETER VOLTAGE VS. TIME 300 AMPERE DISCHARGE AT ROOM TEMP.
18.	COULOMETER VOLTAGE VS. TIME 400 AMPERE DISCHARGE AT ROOM TEMP.
19.	COULOMETER VOLTAGE VS. TIME 500 AMPERE DISCHARGE AT ROOM TEMP.
20.	COULOMETER VOLTAGE VS. TIME 600 AMPERE DISCHARGE AT ROOM TEMP.
21.	CHARGE CONTROL CIRCUIT

I. ABSTRACT

Studies on the effect of plate thickness on sealed cell behavior during high rates of discharge were carried out at 0°F. As in earlier tests, the cell containing the thinner of the two plate sizes used showed the better performance.

Plate impregnation with the high purity nickel and cadmium salt solutions were completed. The plates were formed, and from the plates sealed cells were assembled. These cells, along with controls, were cycled at room temperature, to stabilize their capacities, and then placed in an oven at 120°F to test the charge retention merits of the high purity salts.

Sealed cells using plates with a heavier plate backing support were assembled with 0.025" and 0.034" plates. These cells were used to study the effect of a more uniform plate current distribution on sealed cell behavior during high rates of discharge. The effect of rubidium and cesium as electrolyte additives was also studied under high rate discharge conditions.

A $Cd/Cd(OH)_2$ coulometer, using 0.035" plates was constructed and tested at high current rates. It was found that the capacity of the device decreases with increasing current. It was also found that an excessive amount of heat is generated with this device at high current. Consequently, another one is being tested with thin plates to minimize these undesirable effects.

A breadboard model of the charge control circuit was constructed and tested. The unit functioned properly when activated by a coulometer signal. Three charge control circuits, each capable of handling 110 amperes, were constructed to test each of the three signal generating devices; the coulometer, Adhydrode, and pressure switch.

II. INTRODUCTION

The objectives of this research and development program are to design, develop, and fabricate hermetically sealed, maintenance-free, high rate, nickel-cadmium batteries for aircraft applications. That is, the battery must be capable of delivering the necessary power for engine starting, it must be capable of withstanding the varied environmental conditions that may prevail in an aircraft, and it must be compatible with the constant potential charging system of the aircraft. To achieve these objectives, two broad areas are being investigated.

Firstly, a basic research program has been undertaken with the ultimate goal of improving the electrochemical operation of sealed nickel-cadmium cells. The areas where improvements are sought include longer shelf life, better electrical performance at high rates of charge and discharge, and better electrical performance at high and low temperature extremes.

Secondly, to make the battery compatible with the constant potential charging system of the aircraft, and, at the same time, to eliminate unnecessary overcharging, several methods are being investigated to control battery charging. These methods include monitoring the ampere-hour capacity taken out and put back into the battery (coulometer), the Adhydrode which generates power as pressure is built up inside the cell, and a pressure switch which is triggered by the internal cell pressure.

This report describes the work performed during the third quarter of this program. Details of this work are given in the following sections.

III. BATTERY RESEARCH AND DEVELOPMENT

A. EFFECT OF PLATE THICKNESS ON SEALED CELL BEHAVIOR DURING HIGH RATE CHARGE AND DISCHARGE

Sealed nickel-cadmium cells equipped with pressure gauges and containing 0.020", 0.035" and 0.050" plates were tested to determine the effect of plate thickness (and consequently, current density) on cell behavior during high rates of charge and discharge. In assembling these cells, the total plate volume in each cell was kept as nearly constant as possible to obtain a good comparison in their behavior. All plates were 2.15" x 1.90" and the theoretical capacities of these cells, calculated from the weights of the active material, were 3.23 AH, 3.82 AH and 3.82 AH respectively. The performance of these cells at high rates of charge (up to the 40 ampere rate) and discharge (up to the 60 ampere rate) at room temperature was reported previously (Second Quarterly Technical Progress Report, February 1965).

The high rate performance of these cells was also investigated at low temperature. Cell #1-50 (containing the 0.050" plates) was omitted from these tests because of its poor performance in previous tests. The cells were charged at 400 ma for 16 hours at room temperature, placed in an air-circulated cold chamber and allowed to cool seven hours before discharging. The temperature in the chamber was maintained at $0^{\circ}F\ ^{+5^{\circ}}_{-2^{\circ}}$. Following the seven-hour stand to allow the cell temperatures to equilibrate, the cells were discharged at rates ranging from five amperes to sixty amperes to 0.6 V per cell. Results of these tests are shown in Fig. 1 to 9. The AH capacities obtained at the various discharge rates, and their corresponding current densities, are presented in Table I.

TABLE I

AH CAPACITIES OF SEALED CELLS WITH VARIOUS PLATE THICKNESS AT 0°F.

DISCHARGE RATES	CELL #1-20		CELL #1-35	
	CURRENT DENSITY	CAPACITY	CURRENT DENSITY	CAPACITY
5 amperes	87.5 ma/in.^{2}	1.7 AH	153 ma/in.^{2}	1.75 AH
10 amperes	175 ma/in.^{2}	1.47 AH	306 ma/in.^{2}	1.33 AH
15 amperes	262.5 ma/in.^{2}	1.37 AH	459 ma/in.^{2}	1.12 AH
20 amperes	350 ma/in.^{2}	1.30 AH	612 ma/in.^{2}	0.99 AH
25 amperes	437.5 ma/in.^{2}	1.08 AH	765 ma/in.^{2}	0.64 AH
30 amperes	525 ma/in.^{2}	1.08 AH	918 ma/in.^{2}	0.38 AH
40 amperes	700 ma/in.^{2}	1.0 AH	1224 ma/in.^{2}	0.16 AH
50 amperes	875 ma/in.^{2}	0.93 AH	1530 ma/in.^{2}	*
60 amperes	1050 ma/in.^{2}	0.83 AH	1836 ma/in.^{2}	*

* Cells reached 0.6 V within two seconds from the start of discharge

As may be seen from the data, cell #1-20 (containing the 0.020" plates) again performed better at all discharge rates. Its voltage and capacity were higher. At the fifty ampere and sixty ampere rates, cell #1-35 reached 0.6 V within two seconds from the time the discharge was started.

The better performance of the cell containing the thinner plates is the result of several causes. Firstly, at any given discharge rate, the current density in cell #1-20 is lower. Secondly, because cell #1-20 contains more plates (15 plates in #1-20 and 11 plates in #1-35) within the same space, its internal resistance is lower and consequently, its IR drop is lower. Thirdly, because the center to center spacing of the plates is closer in cell #1-20, its concentration polarization must be lower. The validity of these assumptions is supported by examining the voltage plateaus and AH capacities of the two cells at comparable current densities. At the lower rates (up to about 25 amperes) the two cells yield about the same capacity at comparable current densities. However, at higher rates, where polarization is the predominant cause of voltage and capacity losses, cell #1-20 performed much better at comparable current densities.

Paragraph 3 of the Work Statement specifies a 600 ampere discharge for one minute with the battery voltage maintained at no less than 14 volts. For a 19 cell battery, this means 0.74 volts per cell assuming negligible losses due to the intercell and battery connectors. The experimental results of this section suggest that this requirement can be met at 0°F.

B. EFFECT OF IMPURITIES ON SELF-DISCHARGE OF SEALED NICKEL-CADMIUM CELLS

To study the effect of impurities and the nature of the anionic constituent of the impregnating solution on the self-discharge characteristics of sealed nickel-cadmium cells, high purity nitrates, chlorides, and acetates of nickel and cadmium were prepared. The method of preparation and composition of each of these solutions was described previously (Second Quarterly Technical Progress Report). These solutions were used to impregnate sintered nickel plaques (2.15" x 1.90" x 0.035"). Each impregnation cycle consisted of the following sequence of operations:

1. Absorption of the metal salt solution under vacuum.
2. Drying of the plates at 50°C.
3. Precipitation of the metal in 34% KOH
4. Washing and drying at 50°C.

This impregnation cycle was repeated as many times as was required to achieve the desired weight gain. A summary of the weight gain and the number of cycles required to achieve it for each type of plate is shown in Table II.

TABLE II

WEIGHT GAINS OF SINTERED NICKEL PLAQUES

IMPREGNATING SOLUTION	NO. OF CYCLES REQUIRED	WEIGHT GAIN
Nickel Nitrate	8	23.0 gm/cu. in.
Nickel Chloride	8	23.7 gm/cu. in.
Nickel Acetate	32	21.3 gm/cu. in.
Cadmium Nitrate	5	28.7 gm/cu. in.
Cadmium Chloride	4	28.0 gm/cu. in.
Cadmium Acetate	8	28.0 gm/cu. in.

Because of the low solubility of nickel acetate, 32 cycles were required to achieve a weight gain of 21.3 gm $Ni(OH)_2$/cu. in. using this solution. This represents 92.5% of the desired goal (23 gm/cu. in.). At this point it was felt desirable to terminate plate impregnation because the weight gains per cycle were so small that an additional six to ten cycles might have been required to reach the original goal. In addition, it was also felt that these plates were sufficiently loaded to go ahead with the next phase of these studies.

Following impregnation, the plates were formed. This operation consisted of five charge-discharge cycles at room temperature to stabilize plate capacities prior to sealed cell assembly. Each cell consisted of nine positive and ten negative plates. The cells were charged at 600 ma for 24 hours and discharged at 3.0 amperes. The first and fifth discharge cycles were carried out to -0.5 V to fully discharge both positive and negative plates, while during the other cycles, the discharge was carried out to 1.0 V. Cell capacities were checked to 1.0 V and Hg/HgO reference electrodes were used to ascertain that the cell capacities were positive limiting. The stable capacities obtained from these cells were as follows:

Nitrates	7.95 AH
Chlorides	5.70 AH
Acetates*	8.90 AH

* This cell consisted of ten positive and ten negative plates, so that on a per positive plate basis, the acetates yielded a capacity equal to the nitrates.

Following formation, the plates were thoroughly washed in deionized water and dried. At this time it was noted that the positive plates prepared from the nickel chloride solution showed evidence of a

chemical attack. Apparently, the small traces of chloride left in the plate appear to be deleterious, which may also account for the lower capacity obtained during formation. No evidence of any chemical attack was noted on the other nickel plates or on any of the cadmium plates.

Four nickel plates and six cadmium plates were selected from each group for sealed cell assembly. Two five-plate cells were assembled from each group of plates. Two additional sealed cells were assembled with plates which had been impregnated with standard, battery grade nickel and cadmium nitrates. The two latter cells were added to the group as controls. Each cell, equipped with a pressure gauge, contained 6.5 cc of high purity, 34% KOH as the electrolyte.

The cells were charge-discharge cycled at room temperature until the cell capacities stabilized. The cells were charged at 1.5 amperes for one hour and at 150 ma for 16 hours to insure a complete charge. After a 30 minute stand, the cells were discharged at 750 ma to 1.0 V per cell. Ten such charge-discharge cycles were run to ascertain that the cell capacities had stabilized. The capacities obtained during the last three cycles were averaged and these values are shown in Table III.

TABLE XII

AH CAPACITIES OF HIGH PURITY CELLS

CELL NO.	AH CAPACITY	REMARKS
STN-1	1.41	Control
STN-2	1.43	Control
HPA-1	1.28	Prepared from Acetate
HPA-2	1.44	Prepared from Acetate
HPC-1	1.30	Prepared from Chloride
HPC-2	1.35	Prepared from Chloride
HPN-1	1.43	Prepared from Nitrate
HPN-2	1.41	Prepared from Nitrate

Following room temperature cycling, the cells were charged as above, and placed in an oven maintained at 120°F ± 2°F for seven days. At this writing the cells are in the oven. After a seven-day stand, the cells will be discharged at 750 ma to 1.0 V to determine the charge retention merits of the high purity salts.

C. EFFECT OF RUBIDIUM AND CESIUM ON SEALED CELL BEHAVIOR AT HIGH RATES OF DISCHARGE

In an attempt to obtain a more uniform current distribution in the battery plate and thereby, reduce polarization in the cell during high rates of charge and discharge, sintered nickel plaques with 0.005" nickel as the plate backing support (instead of 0.003") were fabricated. These plaques were fabricated in two sizes: 2.15" x 1.90" for laboratory studies, and 5.90" x 2.75" for assembly of 35 AH prototype cells. Each size plaque was fabricated in 0.025" and 0.034" thickness. These sintered plaques were impregnated with active material and their weight gains are shown in Table IV.

TABLE IV

WEIGHT GAINS OF BATTERY PLATES

PLATE SIZE	$Ni(OH)_2$ gm/cu. in.	$Cd(OH)_2$ gm/cu. in.
2.15" x 1.90" x 0.025"	21.4	27.2
2.15" x 1.90" x 0.034"	23.2	27.2
5.90" x 2.75" x 0.025"	21.6	27.8
5.90" x 2.75" x 0.034"	23.2	27.8

Following active material impregnation, the plates were assembled into flooded, vented cells for electrical formation. Each cell was assembled with nine positive and ten negative plates. Formation consisted of a ten-hour charge rate for 24 hours (240% input) and a two-hour discharge rate to 1.0 V per cell. Table V shows the specific charge and discharge rates, and the stable capacities obtained from these plates.

TABLE V

CHARGE AND DISCHARGE RATES
AND
AH CAPACITIES OF FORMATION CELLS

CELL (PLATE SIZE)	CHARGE RATE	DISCHARGE RATE	CURRENT DENSITY ON DISCHARGE	CAPACITY AH
2.15" x 1.90" x 0.025"	600 ma	3.0 amp	40.8 ma/in^2	5.9
2.15" x 1.90" x 0.034"	800 ma	4.0 amp	54.5 ma/in^2	8.0
5.90" x 2.75" x 0.025"	2.0 amp	10.0 amp	34.2 ma/in^2	22.3
5.90" x 2.75" x 0.034"	3.0 amp	15.0 amp	51.4 ma/in^2	31.8

The larger plates were set aside for fabricating 35 AH prototype cells. The smaller plates were assembled into two groups of sealed cells. One group of cells was assembled with eleven 0.034" plates (five positives and six negatives) and 13 cc of electrolyte. The other group was assembled with thirteen 0.025" plates (six positives and seven negatives) and 14 cc of electrolyte. The electrolyte used was 34% KOH. However, to some cells, electrolyte was added containing ten mole percent of rubidium hydroxide, and to some cells, electrolyte was added containing ten mole percent of cesium hydroxide. The make-up of these electrolyte solutions was as follows:

KOH	28.2%
RbOH	5.8%

KOH	26.2%
CsOH	7.8%

Thus, each group consisted of four cells with the following electrolyte combinations:

Two cells with 34% KOH

One cell with 34% KOH containing RbOH

One cell with 34% KOH containing CsOH

All cells were first charge-discharge cycled at room temperature. The cells were charged at 400 ma for twenty hours and discharged at two amperes to 1.0V per cell. The capacities of these cells are shown in Table VI.

Following the low rate discharging, the cells were charged as before and discharged at sixty amperes at room temperature. These data are shown in Figures 10 to 12.

Figure 10 shows data for cells containing 34% KOH. Figure 11 shows data for cells with CsOH in the electrolyte, and Figure 12 shows data for cells with RbOH in the electrolyte.

TABLE VI

AH CAPACITIES OF CELLS AT THE 2A RATE
CONTAINING ELECTROLYTE ADDITIVES

CELL NO.	CAPACITY, AH	REMARKS
1-255AD	3.10	0.025" plates, 34% KOH
2-255AD	3.17	0.025" plates, 34% KOH
3-255AD	3.07	0.025" plates, 10% CsOH
4-255AD	3.0	0.025" plates, 10% RbOH
1-345AD	3.24	0.034" plates, 34% KOH
2-345AD	3.40	0.034" plates, 34% KOH
3-345AD	3.24	0.034" plates, 10% CsOH
4-345AD	3.30	0.034" plates, 10% RbOH

TABLE VII

AH CAPACITIES OF CELLS
AT 60 AMPERE DISCHARGE RATE

	0.025 PLATES		0.034" PLATES	
ELECTROLYTE	CURRENT DENSITY	CAPACITY, AH	CURRENT DENSITY	CAPACITY, AH
34% KOH	1.22A/in^2	2.03	1.47 A/in^2	1.06
KOH + CsOH	1.22 A/in^2	1.60	1.47 A/in^2	1.0
KOH + RbOH	1.22 A/in^2	1.49	1.47 A/in^2	0.84
34% KOH *	1.05 A/in^2	1.5	1.836 A/in^2	1.0

* Cells #1-20 and #1-35

The data are also tabulated in Table VII, and for comparison, the data obtained for cells #1-20 and #1-35 under comparable conditions are also included.

As in previous experiments, the cells containing the thinner plates showed the better performance at the high discharge rates. It is interesting to compare results obtained earlier at the same discharge rate under comparable conditions. The data indicate that while the heavier plate backing support has no apparent effect on the high rate performance of the heavier plate, it does, however, show an improvement with the thinner plates. Apparently, the more uniform current distribution in the heavier plate is overshadowed by other effects, namely, polarization. However, in the thinner plate cells, where polarization is reduced, the more uniform current distribution shows a definite advantage.

To show the effect of the electrolyte additives on cell performance at the high discharge rate, data for the 0.025" plate cells were plotted as shown in Figure 13. As may be seen, the cells containing the electrolyte additives have a lower voltage and a lower capacity. Experiments are now in progress to measure the resistivities of these solutions to determine if this is the cause of these observations.

IV. BATTERY CHARGE CONTROL

A. COULOMETER CHARGE CONTROL

To investigate its high rate characteristics, a $Cd/Cd(OH)_2$ coulometer was constructed. Ten plates, each 5.90" x 2.75" x .035", were used for each electrode. The device was conditioned to place its electrodes in their proper states of charge, and then cycled several times, at 10 amperes, to stabilize its capacity. A typical "charge-discharge" curve is shown in Figure 14.

The effects of high current rates on the coulometer were investigated by subjecting it to charges and discharges ranging from 100 amperes to 600 amperes in 100 ampere intervals. These data are shown in Figures 15 to 20. The ampere-hour capacity of the coulometer decreases as the rate is increased in a manner similar to the behavior of a nickel-cadmium cell. This behavior is desirable, for if the coulometer becomes unbalanced with respect to the battery, it could either prevent complete charging by giving a premature signal, or cause excessive overcharging by giving a delayed signal. To insure safe charging, it becomes desirable to have the coulometer give a slightly premature signal at all charging rates.* During the course of these experiments, it was noted that as the current was increased, the coulometer got increasingly warmer. At 600 amperes, it became so hot that water vapor appeared to be boiling off through the vent.

* It might be noted that, at 600 amperes the coulometer had an average voltage drop of 0.7 volt for the first minute of discharge.

A $Cd/Cd(OH)_2$ coulometer employing 0.025" plates was, therefore, constructed to determine if an increase in capacity at high rates, similar to the increase obtained using thin plates in nickel-cadmium cells, would result, and at the same time reduce the amount of heat generated due to I^2R. The coulometer was filled with 34% KOH until it became slightly over-saturated, and then the excess electrolyte was removed. It was found that a coulometer with a limited amount of electrolyte cannot be conditioned, so it became necessary to flood the device in order to place its electrodes in their proper states of charge. It is believed that oxygen evolving from the anode and recombining with the cathode is the mechanism that prevented the conditioning of the coulometer in its semi-dry state. The coulometer is now undergoing conditioning in the flooded state. After conditioning, the excess electrolyte will be removed, and the cell will be sealed prior to high rate testing.

B. CHARGE CONTROL CIRCUIT

A schematic diagram of the charge control circuit is shown in Figure 21. The circuit operates as follows: Transistor T_1 and T_2 form a Schmitt trigger. With no input signal, T_2 is conducting and T_1 is non-conducting. Thus, point C is at a high potential with respect to ground. This causes the unijunction transistor, UJ_2, to oscillate and send current pulses into the gate of the silicon controlled rectifier, SCR_1. If a charger with the polarity shown is connected between terminals A and B, current will flow in a direction to charge the battery if the charger voltage is greater than the battery voltage. This current will flow through SCR_1 because it has been turned on by UJ_2. Point D is at almost zero potential with respect to ground, and therefore, UJ_1 is not oscillating. Capacitor, C, will charge to the voltage of the battery through Resistor R. When the signal voltage reaches a selected value, transistor T_1 will turn on and T_2 will turn off. This action is regenerative. This makes point C

a low potential with respect to ground and causes UJ_2 to stop oscillaing. Point D, now being at a high potential, starts UJ_1 oscillating and current flowing into the gate of SCR_2. SCR_2 is turned on and the capacitor, C, is connected across the terminals of SCR_1 thereby reversing the polarity of the voltage across SCR_1 and turning it off. SCR_2 cannot stay on because after the capacitor discharges, the only current that could flow must flow through R which has a resistance high enough to keep this current below the minimum holding current of SCR_2. When the signal voltage decreases to a selected value, SCR_1 is again turned on and charging is resumed. The silicon rectifier, SR, is employed to allow the battery to be discharged by any load placed across terminals A and B.

This circuit can be used with either the coulometer, pressure switch or amplified Adhydrode signal as a means of control. Many of the problems associated with this circuit were concerned with designing a Schmitt trigger to operate with the coulometer and the Adhydrode. This is because near the end of charge, the Adhydrode and coulometer voltage both rise slowly, from an electronic point of view, and at a certain voltage level the cell is fully charged. At this voltage, transistor T_2 should switch from its on state to its off state and turn SCR_2 completely on before capacitor C discharges appreciably. The first breadboard of this circuit had a slow response time, and, therefore, work was concentrated on designing a Schmitt trigger with a fast turn on time.

A prototype charge control circuit capable of handling charging currents of 16 amperes and discharging currents of 6 amperes was tested by using it in conjunction with a coulometer, to control the charging of a fifteen-cell, 35 AH battery. A typical cycle ran as follows: the cells were discharged for 1½ hours, then the load was disconnected and a constant potential source was connected to the battery. The charger remained

connected to the battery until the coulometer gave a signal to the charge control circuit to terminate charging current. Twelve cycles were run, and the charge control circuit functioned properly upon signal from the coulometer.

On the basis of the successful operation of this control circuit, three circuits were built. Each of these circuits is capable of handling charging currents of 110 amperes. These circuits will be used to evaluate each of the three methods of determining end of charge. Three groups of cells will be cycled, with their charging cycles controlled by the coulometer, Adhydrode, and pressure switch. Pressure at the end of charge and ampere-hour capacity will be recorded and evaluated to determine the best method of charge control.

V. CONCLUSIONS

Studies on the effect of plate thickness on sealed cell behavior showed that thin-plate cells performed better at high rates. The improved performance of such cells is the result of reduced polarization, which is the predominant factor in determining cell voltage and capacity at high rates.

A heavier plate backing support (and consequently, a more uniform plate current distribution) appears to have a greater effect on thin-plate cells when such cells are discharged at high rates.

A $Cd/Cd(OH)_2$ coulometer, at high rates, behaves similarly to a nickel-cadmium cell, and an average voltage drop of 0.7 volt can be expected from a coulometer constructed with 0.035" plates, during the first minute of a 600 ampere discharge.

A breadboard model of the charge control circuit functioned properly, at medium currents, showing that the basic design of the circuit is correct.

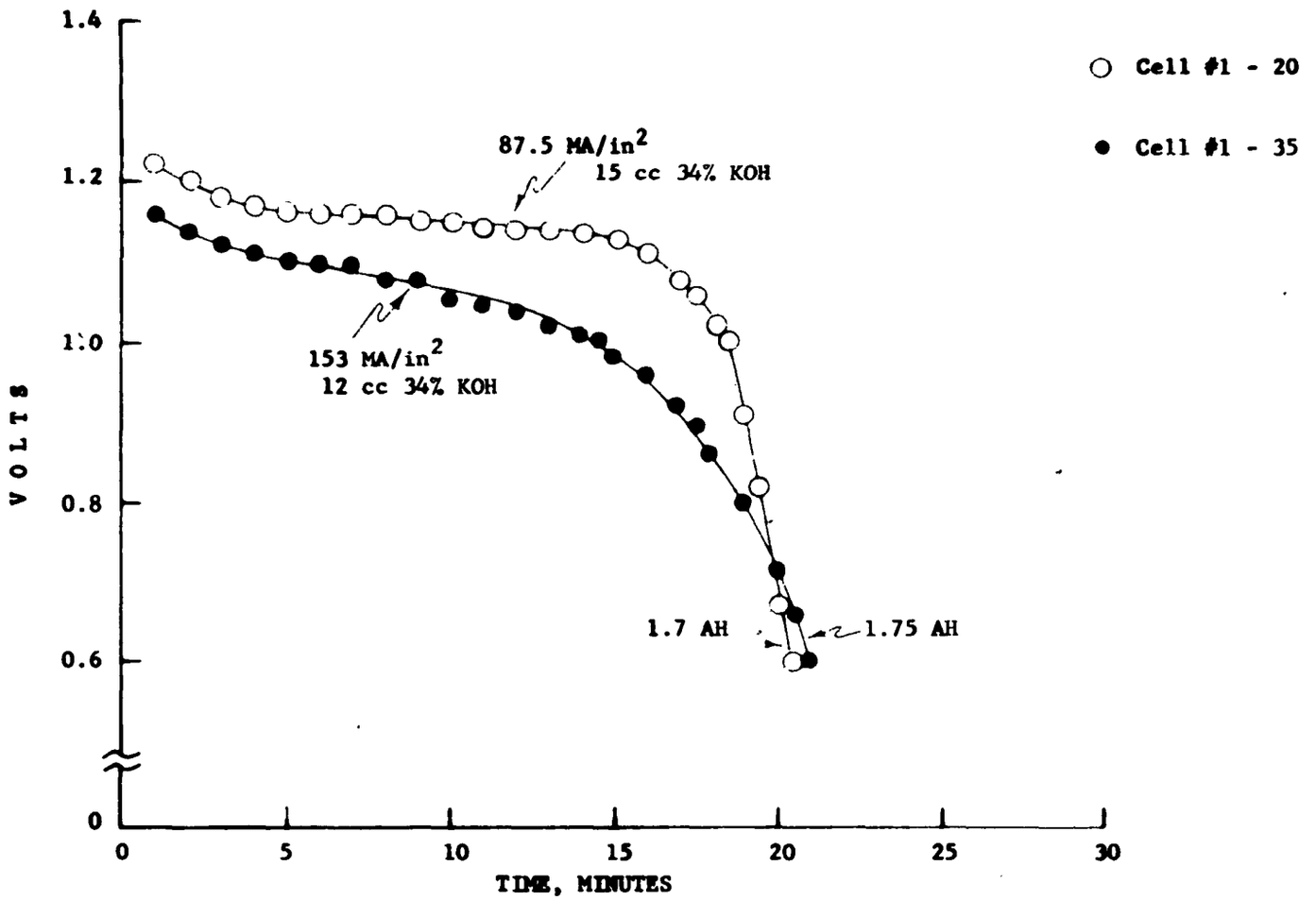

FIGURE 1 - VOLTAGE VS. TIME
5 AMP. DISCHARGE AT 0°F
400 MA CHARGE 16 HRS. AT R.T.

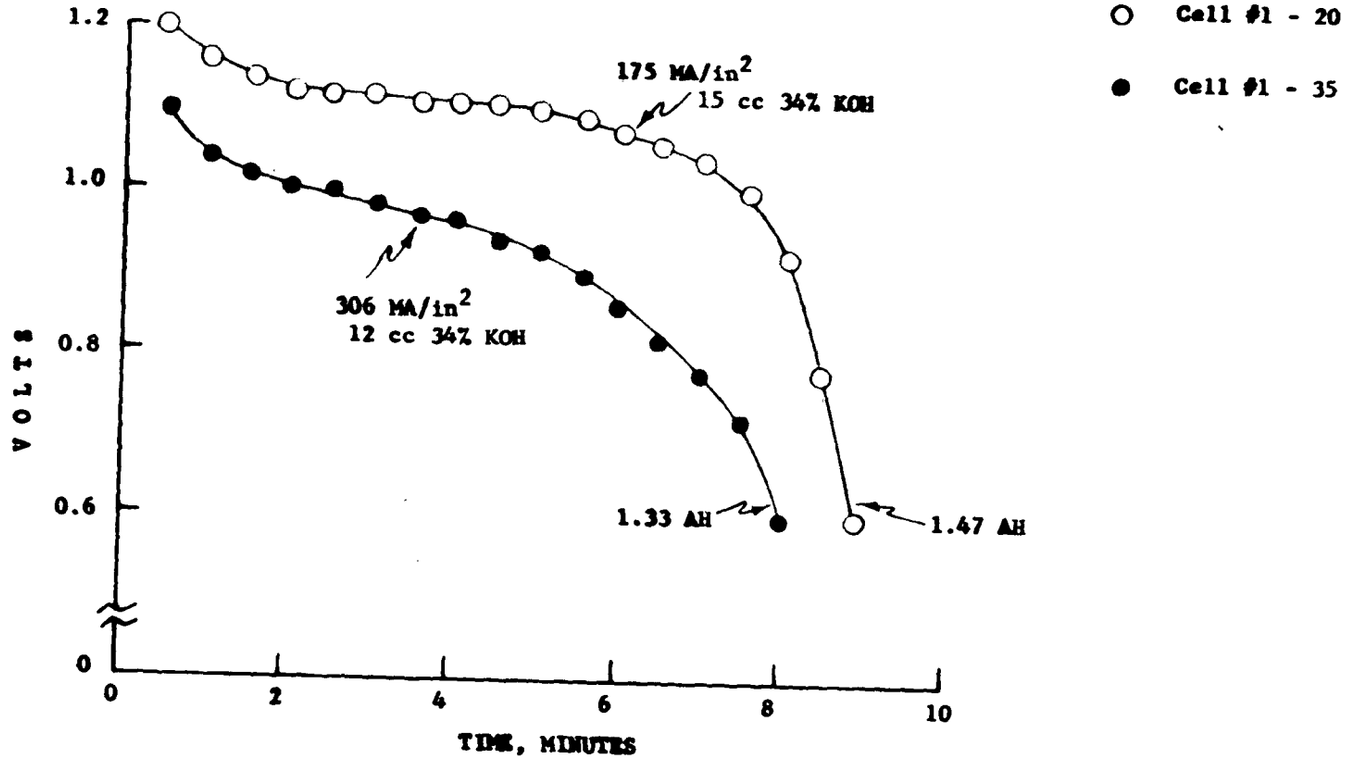

FIGURE 2 - VOLTAGE VS. TIME
10 AMP. DISCHARGE AT 0°F
400 MA CHARGE 16 HRS. AT R.T.

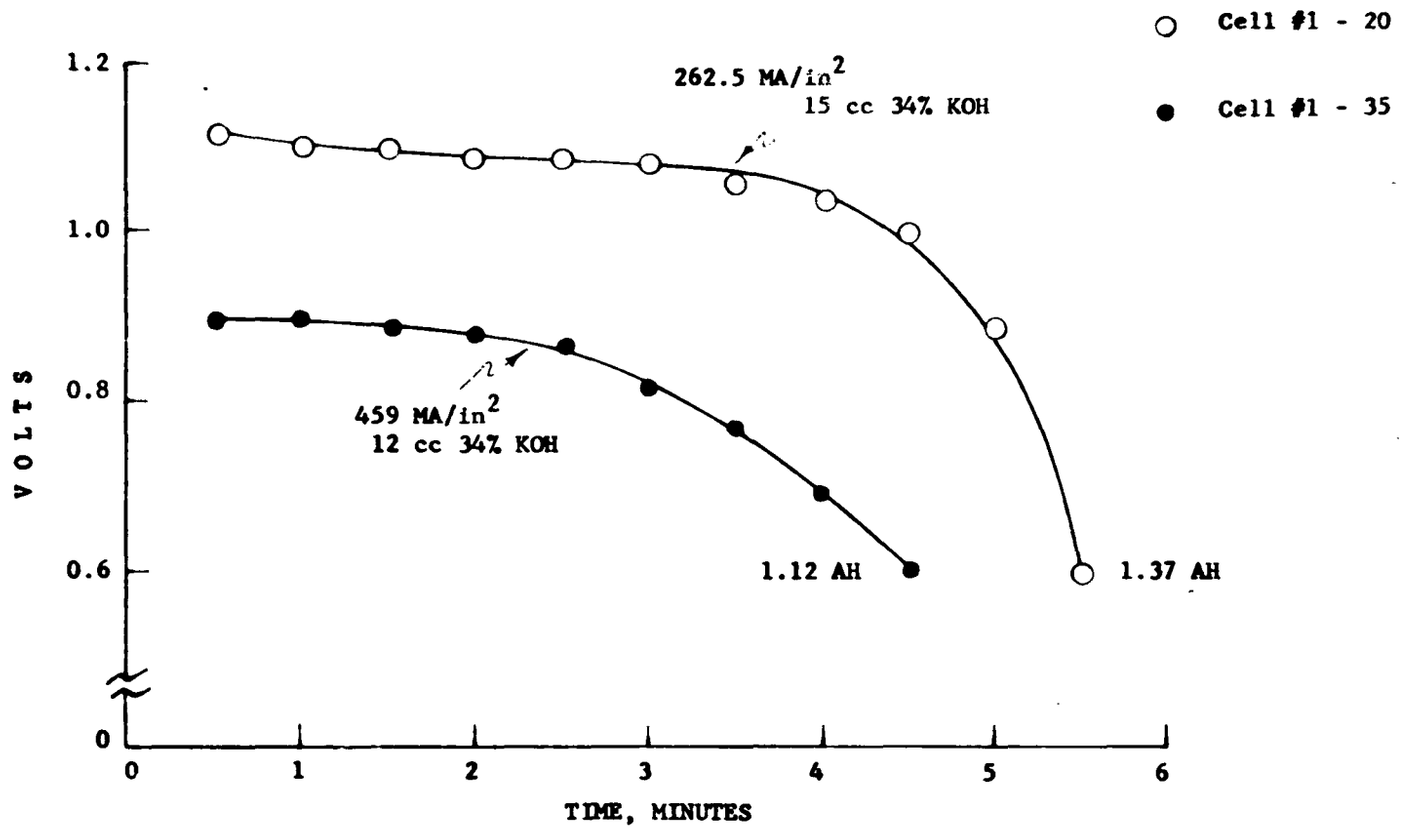

FIGURE 3 - VOLTAGE VS. TIME
15 AMP. DISCHARGE AT 0°F
400 AM CHARGE 16 HRS. AT R.T.

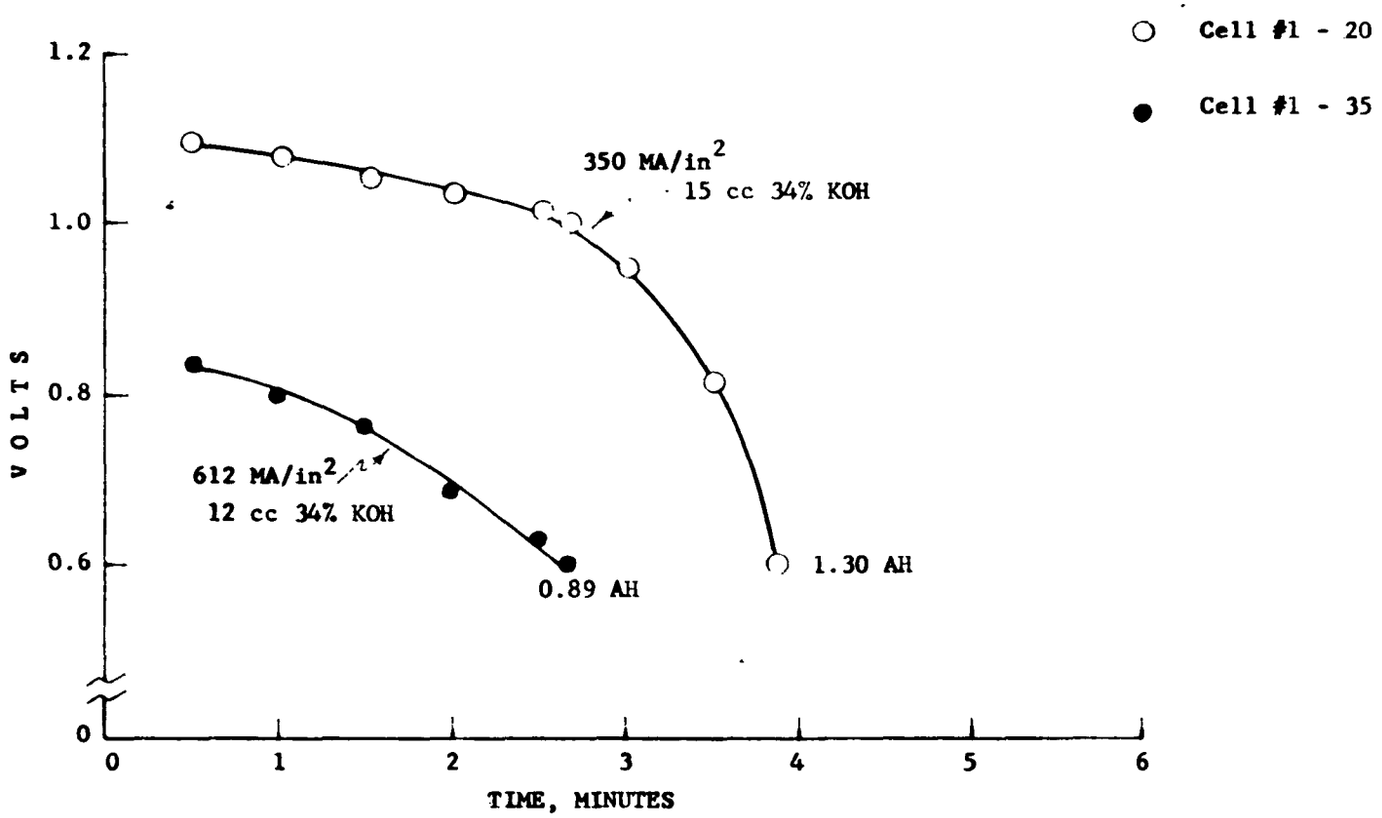

FIGURE 4 - VOLTAGE VS. TIME
20 AMP. DISCHARGE AT 0°F
400 MA CHARGE 16 HRS. AT R.T.

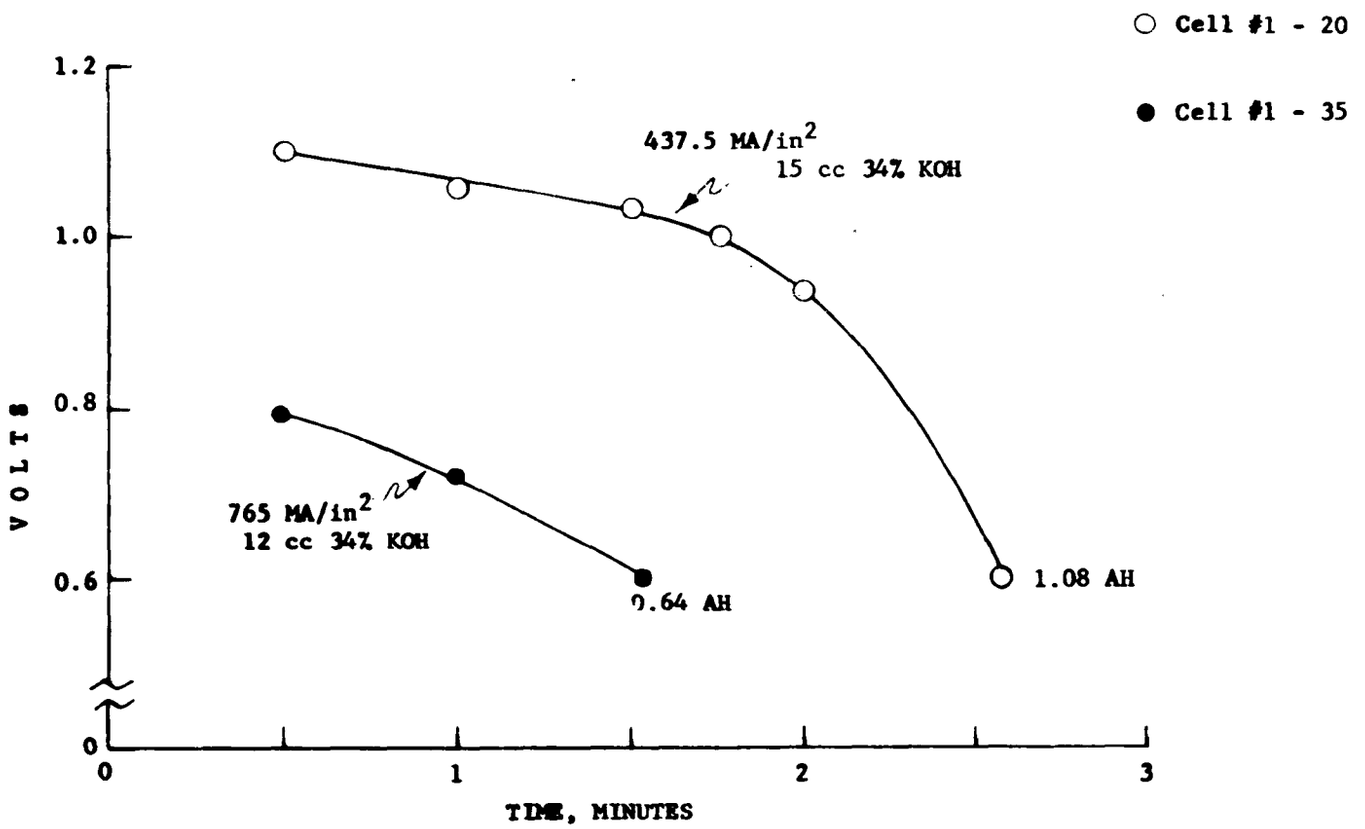

FIGURE 5 - VOLTAGE VS. TIME
25 AMP. DISCHARGE AT 0°F
400 MA CHARGE 16 HRS. AT R.T.

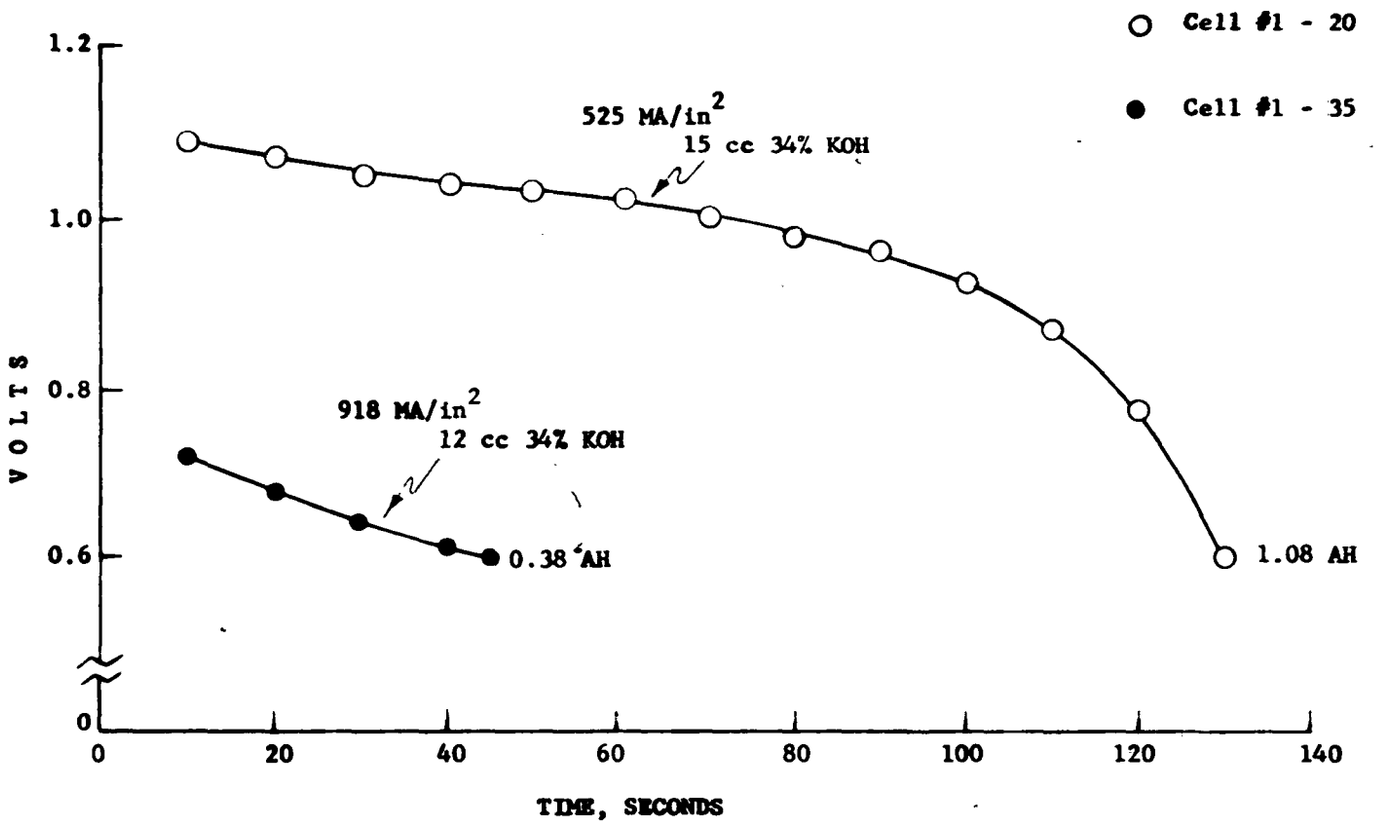

FIGURE 6 - VOLTAGE VS. TIME
30 AMP. DISCHARGE AT 0°F
400 MA CHARGE 16 HRS. AT R.T.

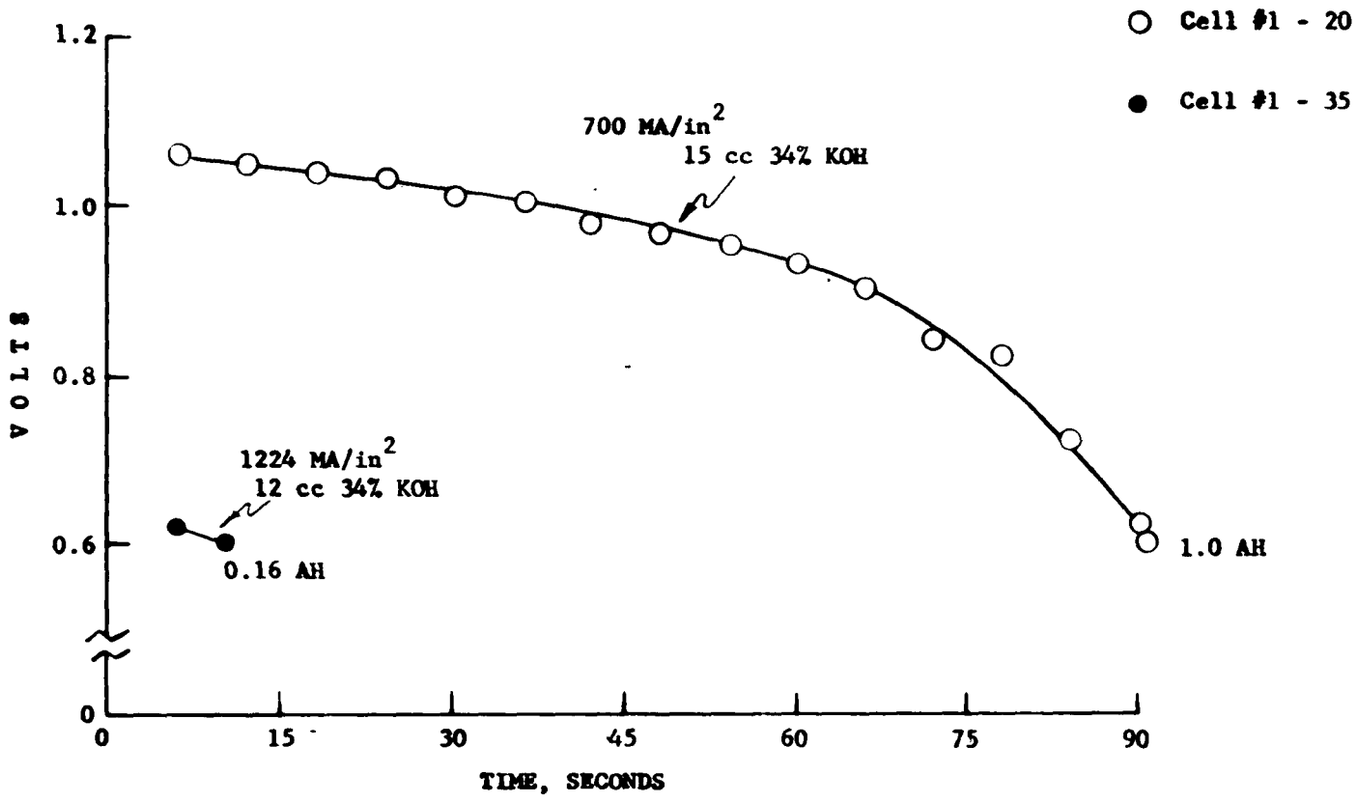

FIGURE 7 - VOLTAGE VS. TIME
40 AMP. DISCHARGE AT 0°F
400 MA CHARGE 16 HRS. AT R.T.

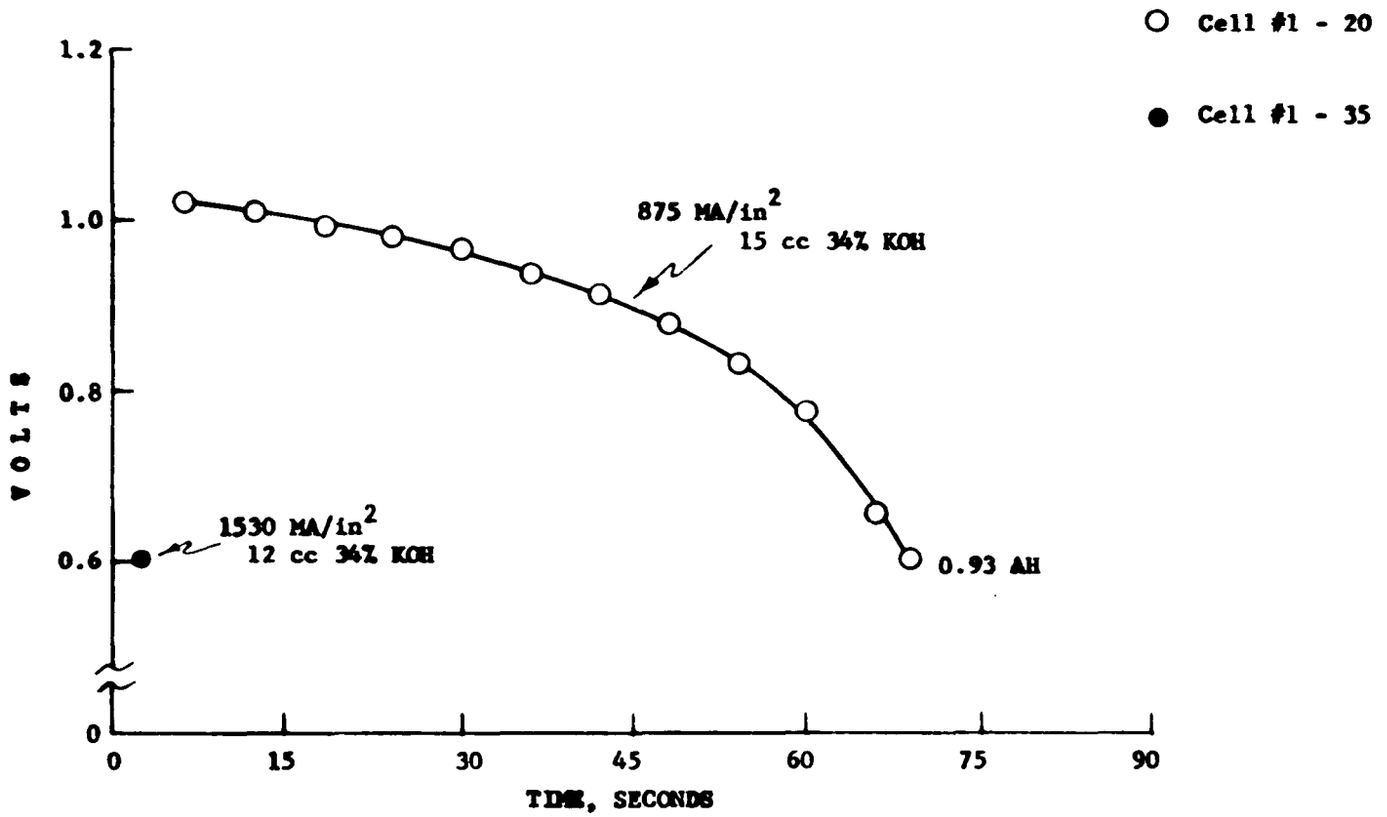

FIGURE 8 - VOLTAGE VS. TIME
50 AMP. DISCHARGE AT 0°F
400 MA CHARGE 16 HRS. AT R.T.

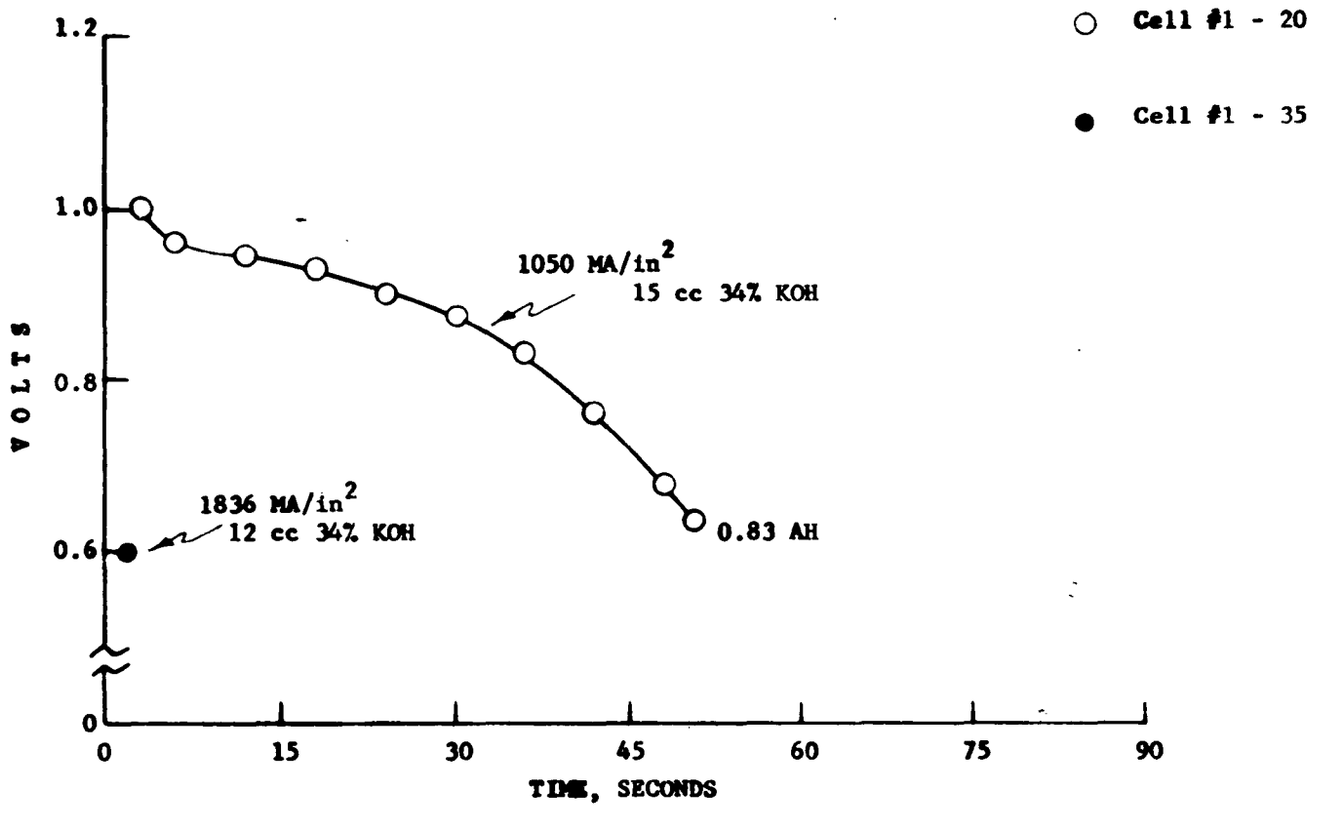

FIGURE 9 - VOLTAGE VS. TIME
60 AMP. DISCHARGE AT 0°F
400 MA CHARGE 16 HRS. AT R.T.

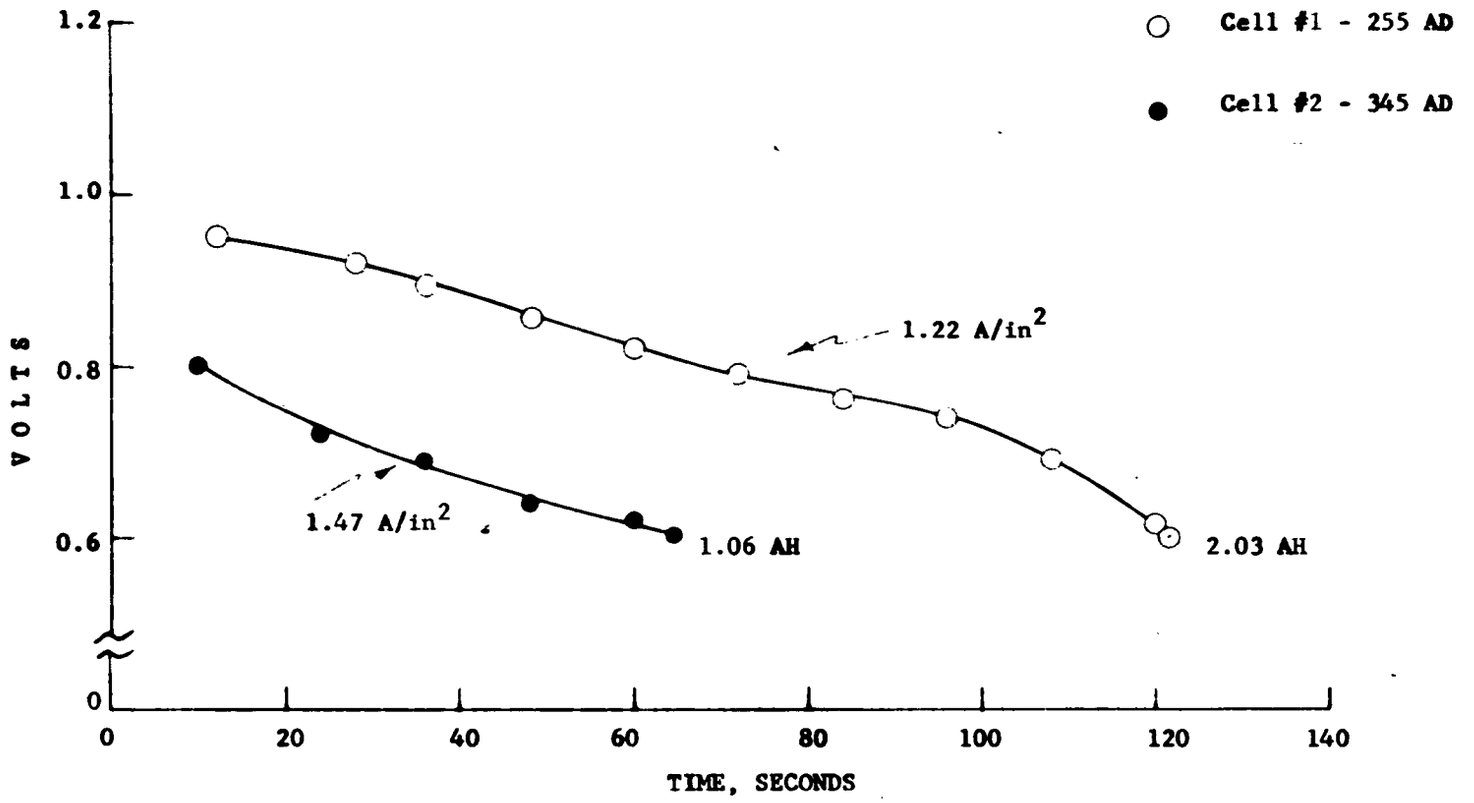

FIGURE 10 - VOLTAGE VS. TIME
60 AMP. DISCHARGE AT R.T.
400 MA CHARGE AT R.T.

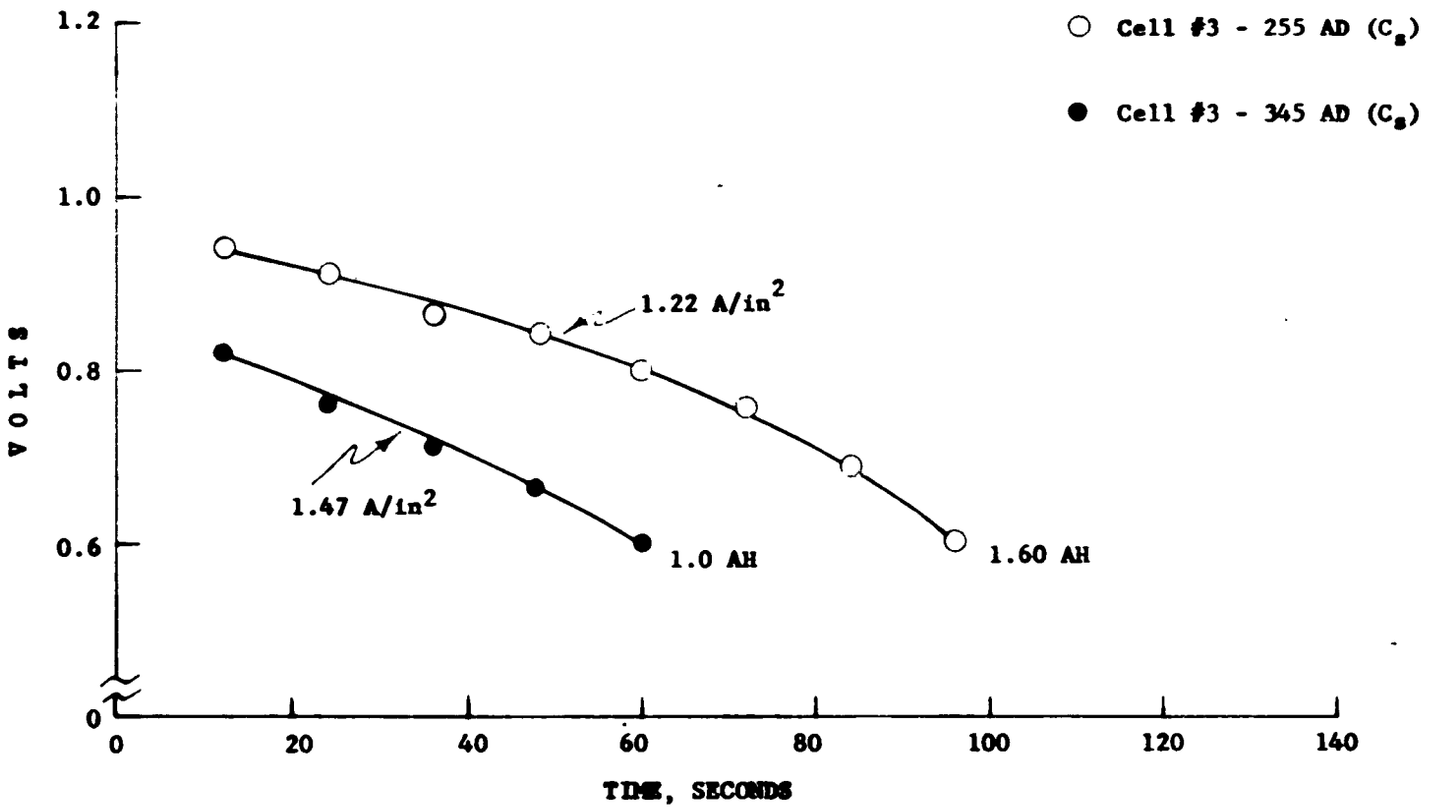

FIGURE 11 - VOLTAGE VS. TIME
60 AMP. DISCHARGE AT R.T.
400 MA CHARGE AT R.T.

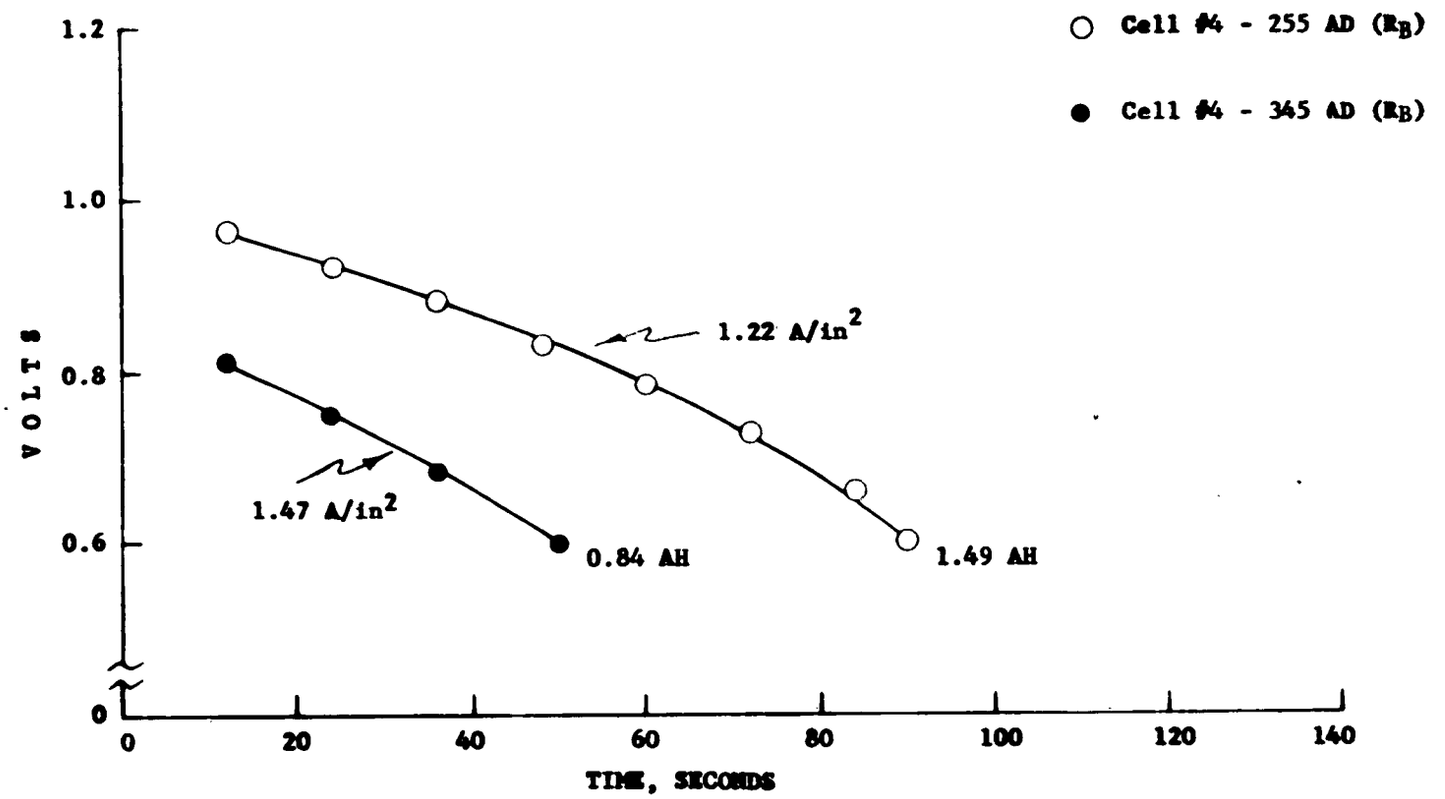

FIGURE 12 - VOLTAGE VS. TIME
60 AMP. DISCHARGE AT R.T.
400 MA CHARGE AT R.T.

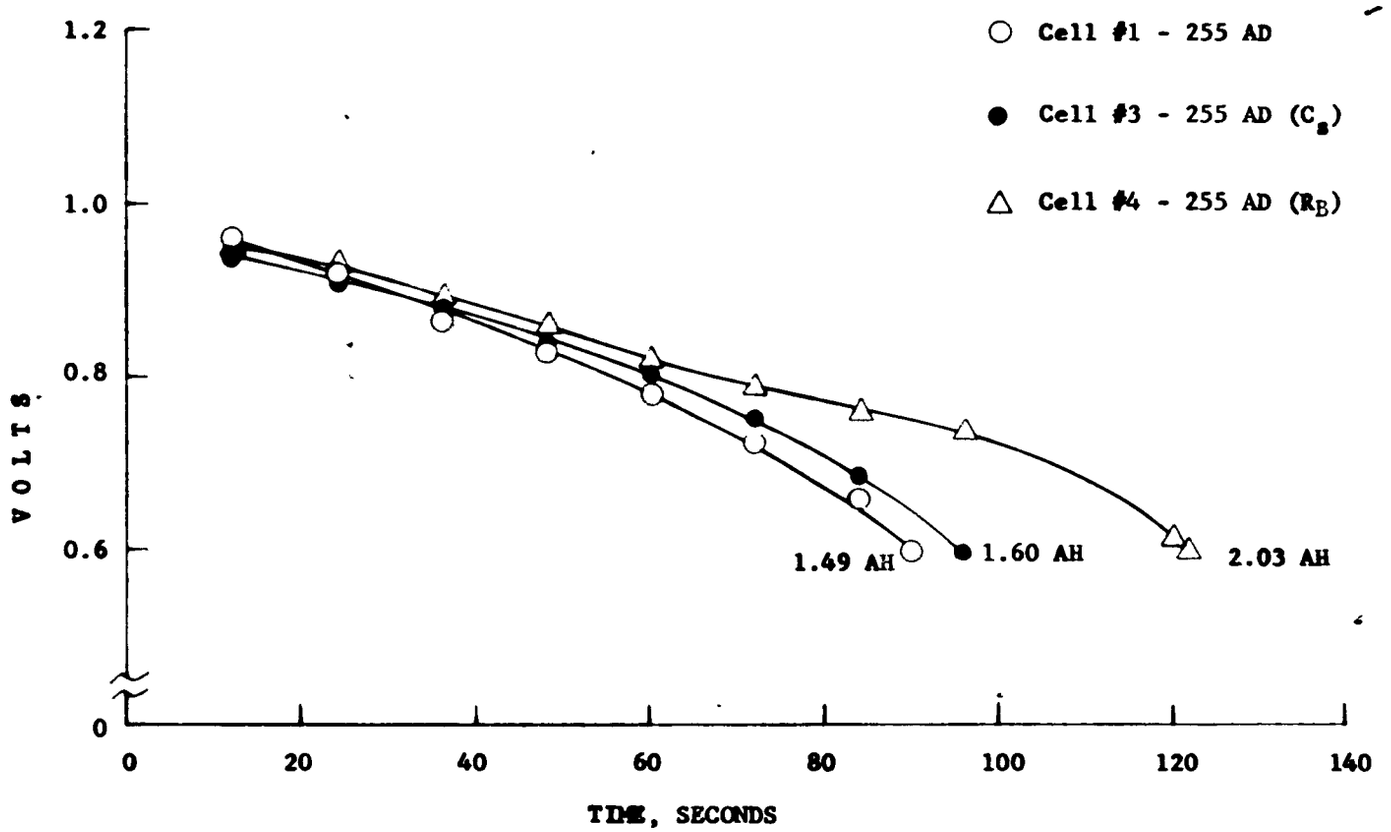

FIGURE 13 - EFFECT OF RUBIDIUM AND CESIUM ON CELL VOLTAGE AND CAPACITY AT HIGH DISCHARGE RATE (20C)

60 AMP. DISCHARGE AT R.T. (1.22 A/in^2)
400 MA CHARGE AT R.T.

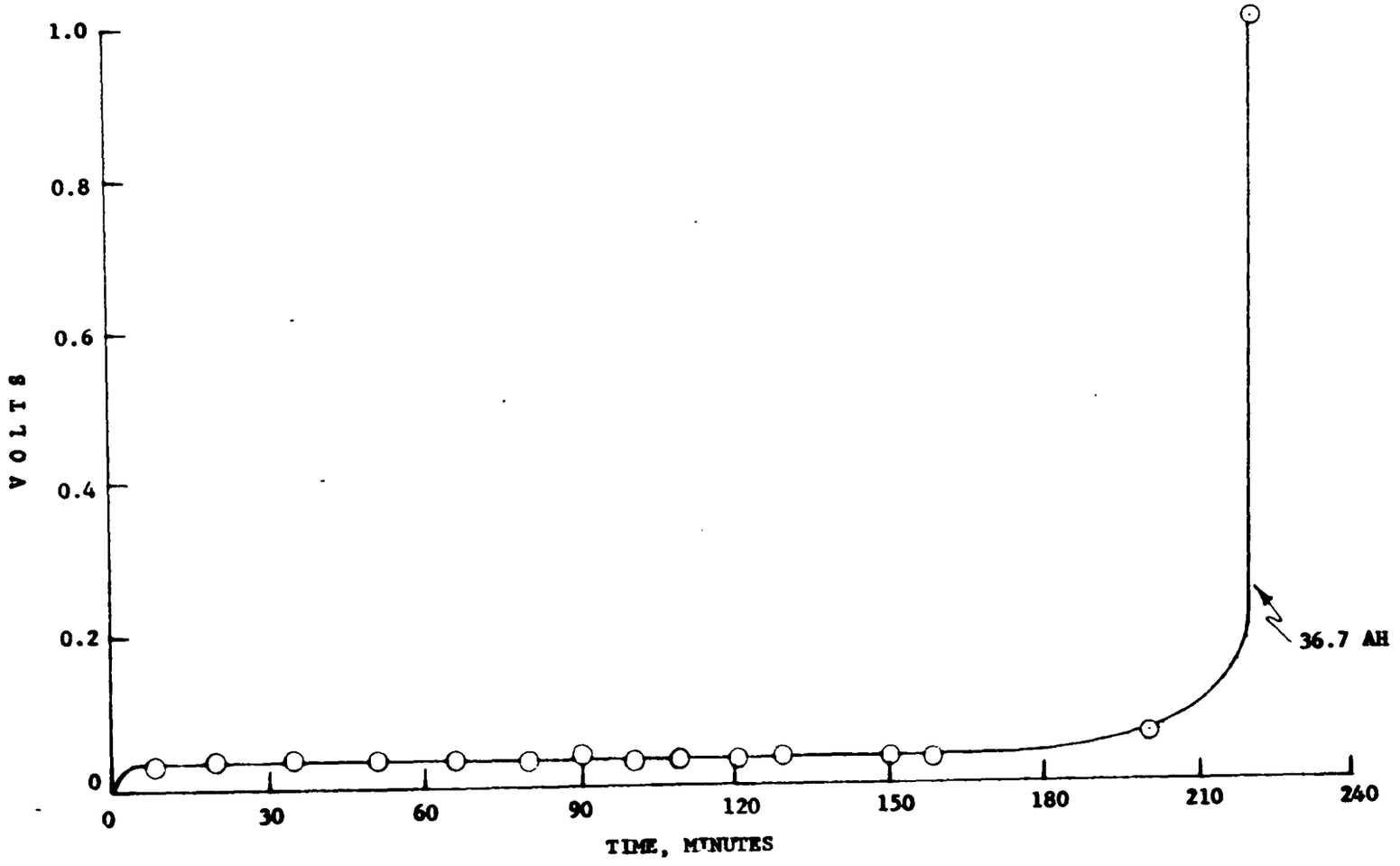

FIGURE 14 - COULOMETER VOLTAGE VS. TIME
10 AMP. DISCHARGE AT ROOM TEMPERATURE
(30.8 MA/in^2)

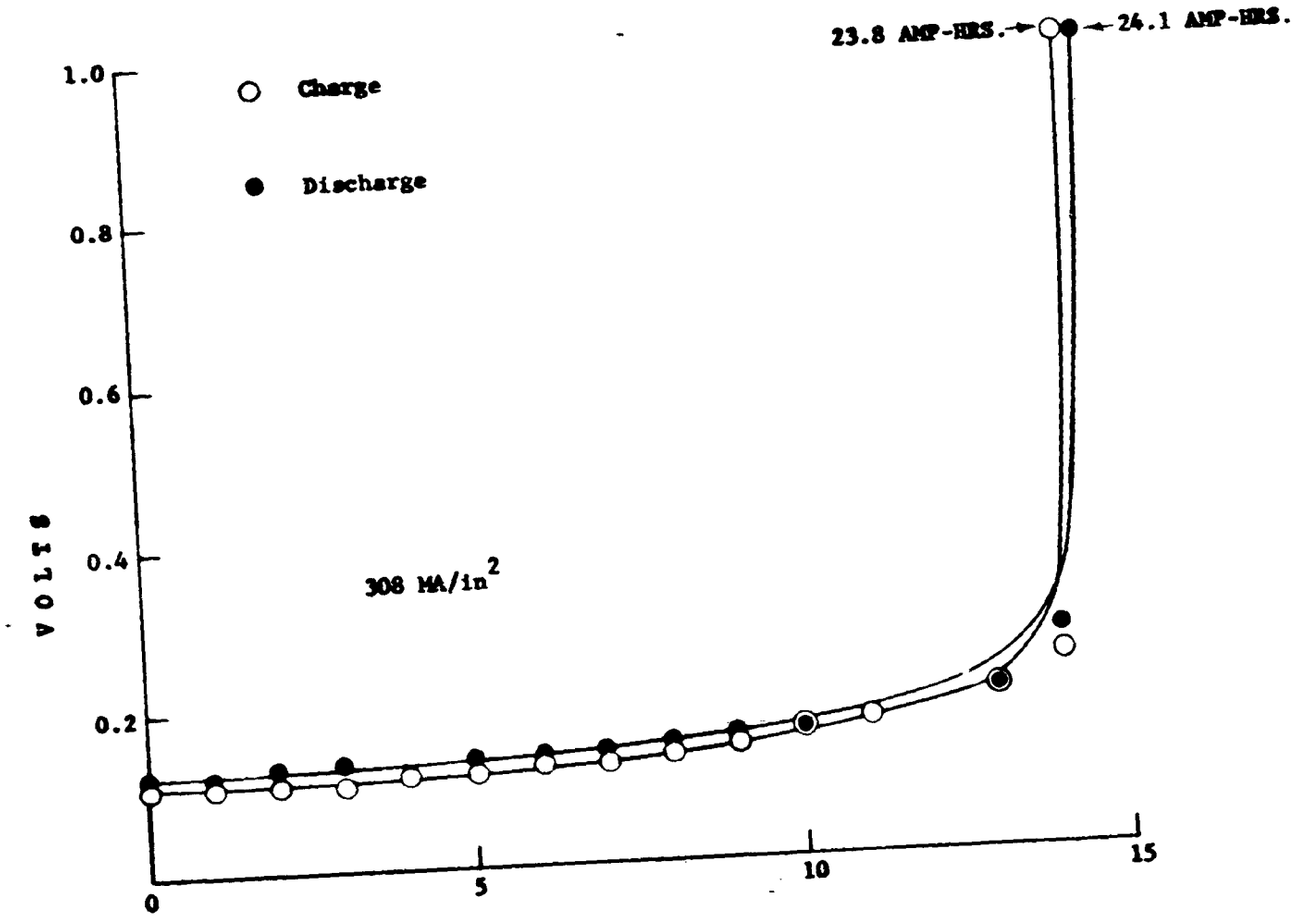

FIGURE 15 - COULOMETER VOLTAGE VS. TIME FOR 100 AMPERE CHARGE AND DISCHARGE AT ROOM TEMPERATURE

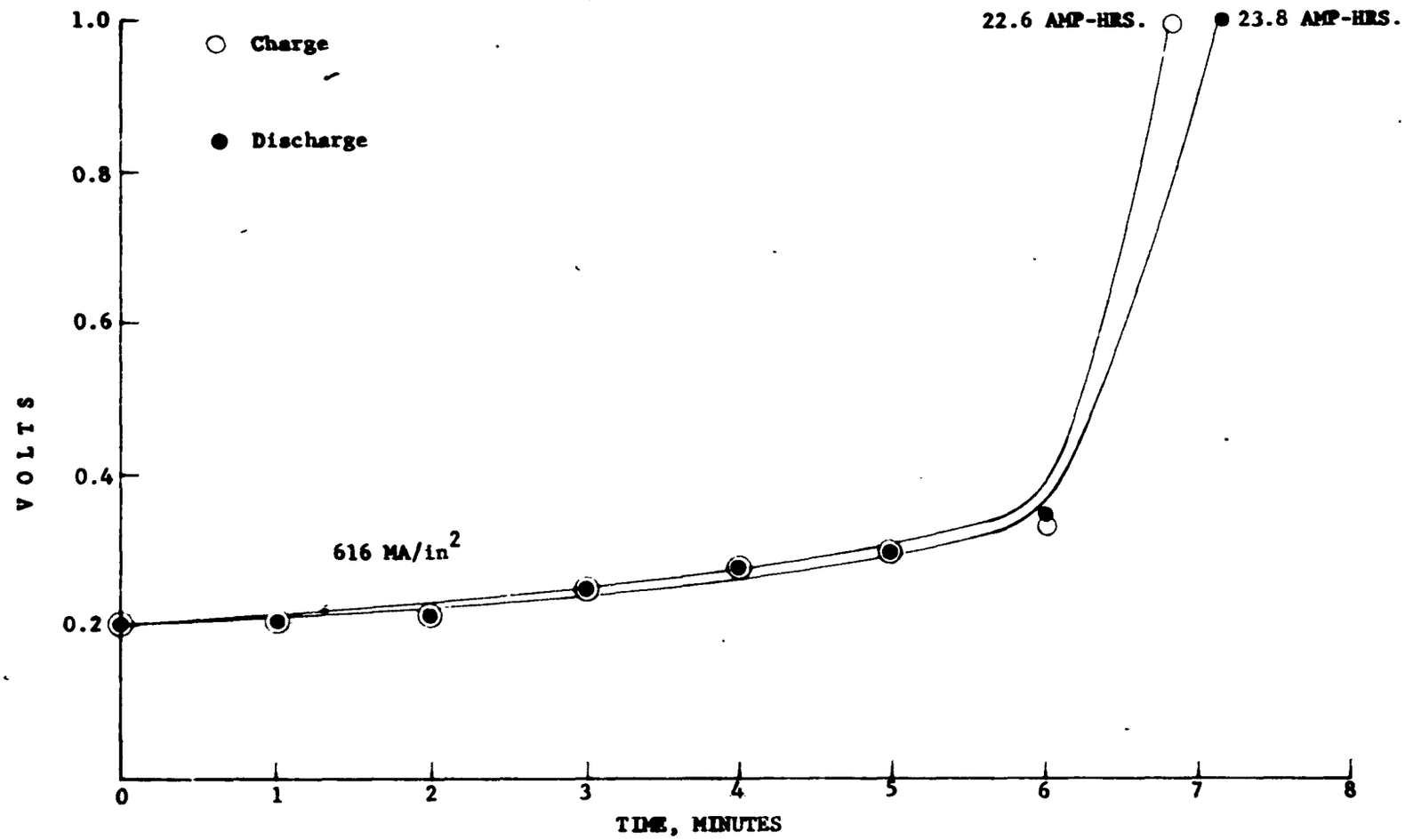

FIGURE 16 - COULOMETER VOLTAGE VS. TIME FOR 200 AMPERE CHARGE AND DISCHARGE AT ROOM TEMPERATURE

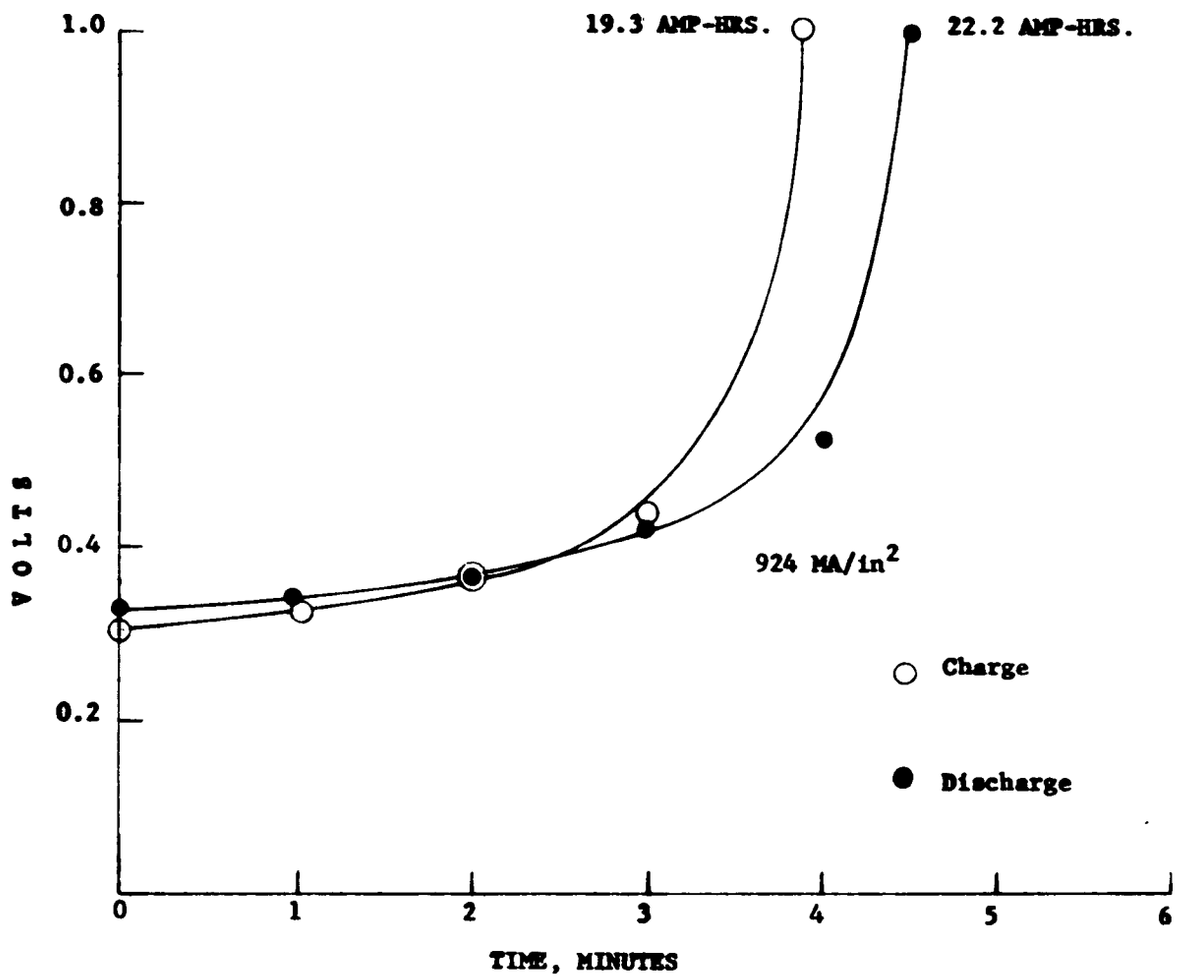

FIGURE 17 - COULOMETER VOLTAGE VS. TIME FOR 300 AMPERE CHARGE AND DISCHARGE AT ROOM TEMPERATURE

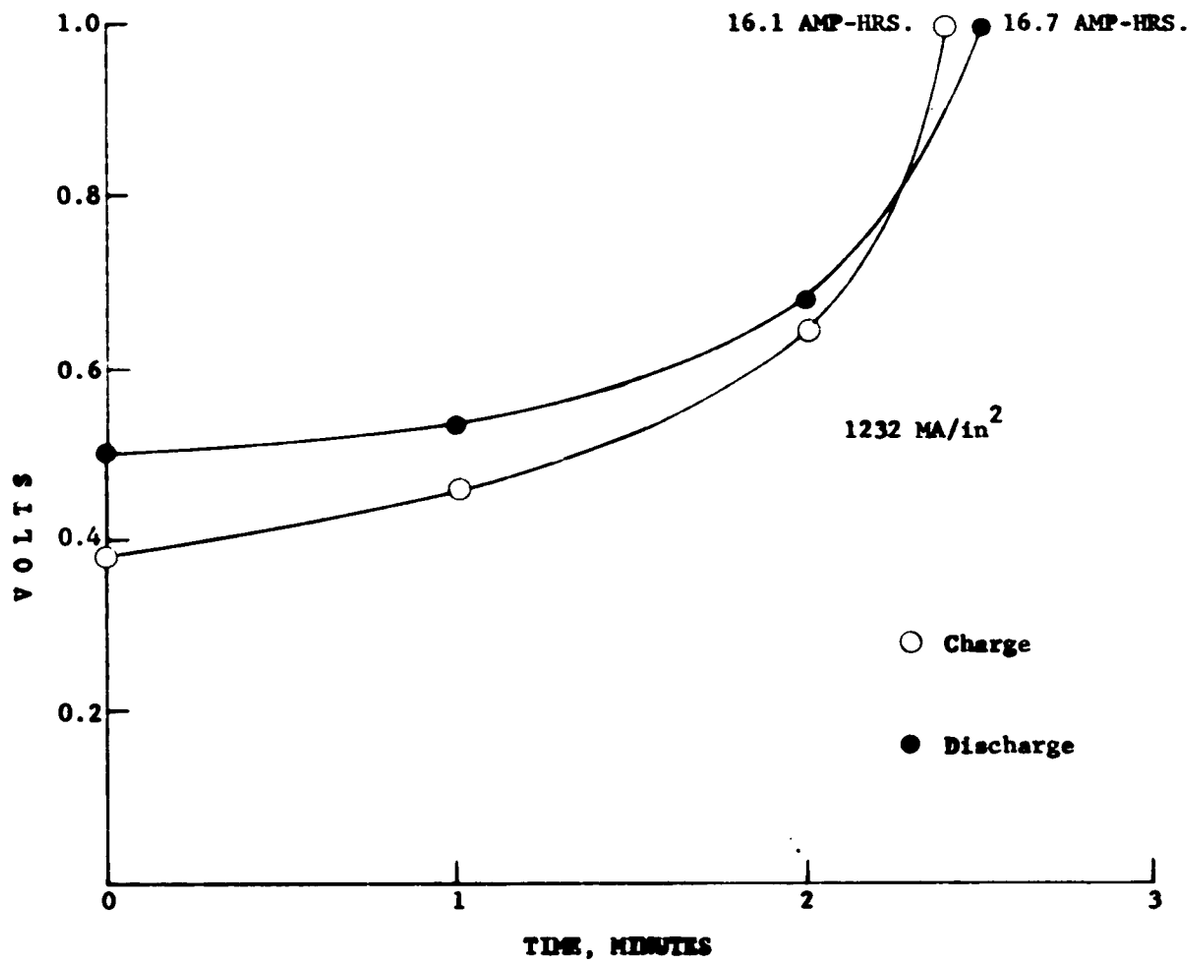

FIGURE 18 - COULOMETER VOLTAGE VS. TIME FOR 400 AMPERE CHARGE AND DISCHARGE AT ROOM TEMPERATURE

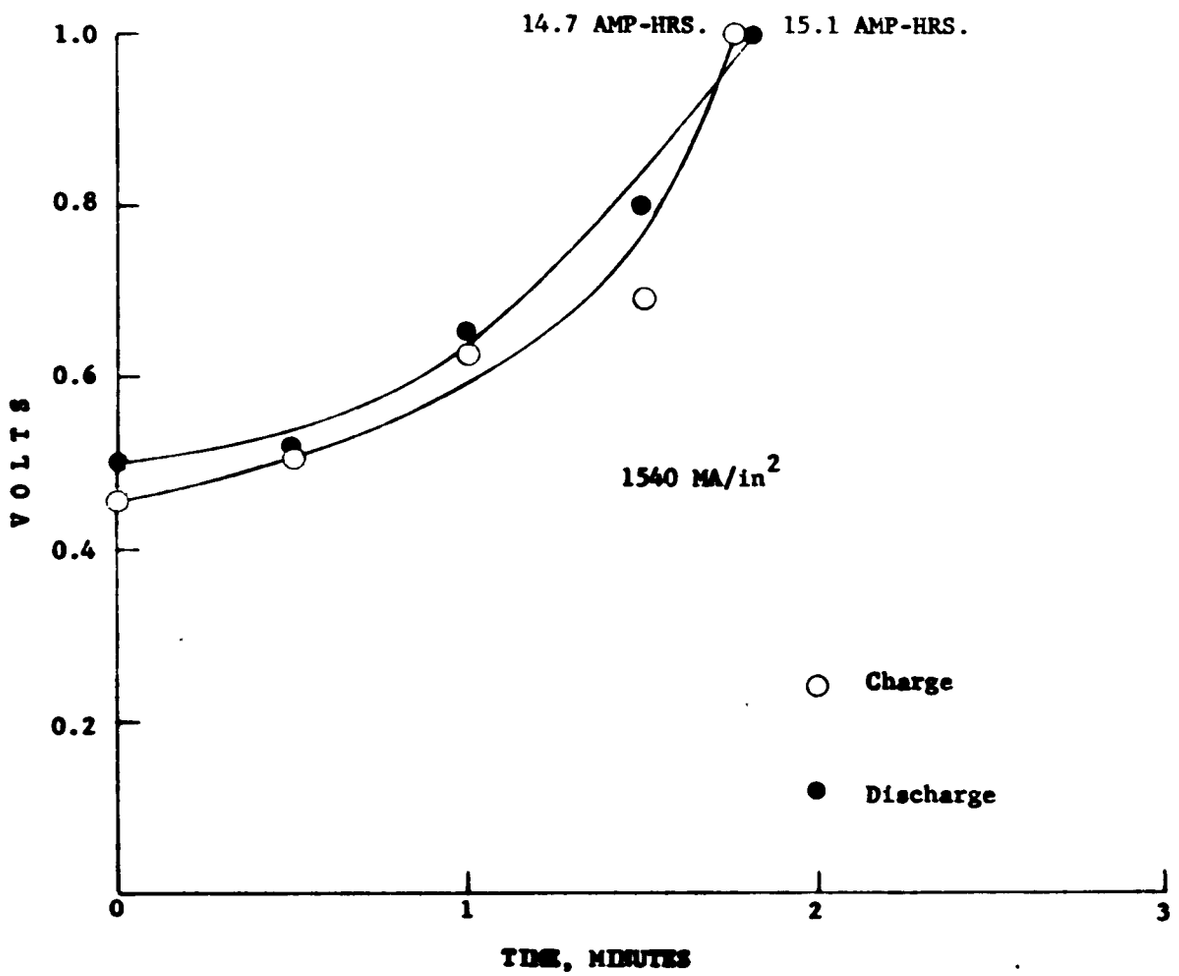

FIGURE 19 - COULOMETER VOLTAGE VS. TIME FOR 500 AMPERE CHARGE AND DISCHARGE AT ROOM TEMPERATURE

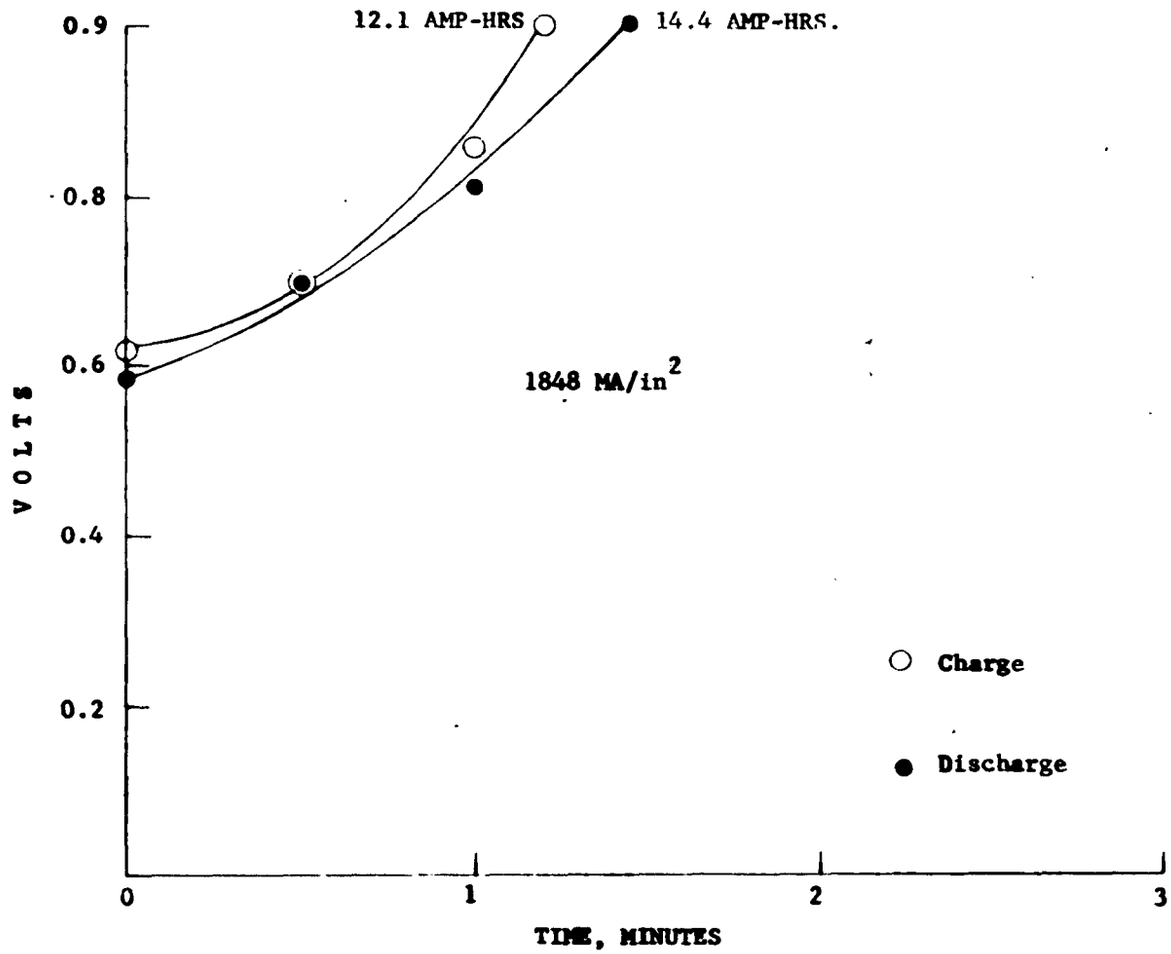

FIGURE 20 - COULOMETER VOLTAGE VS. TIME FOR 600 AMPERE CHARGE AND DISCHARGE AT ROOM TEMPERATURE

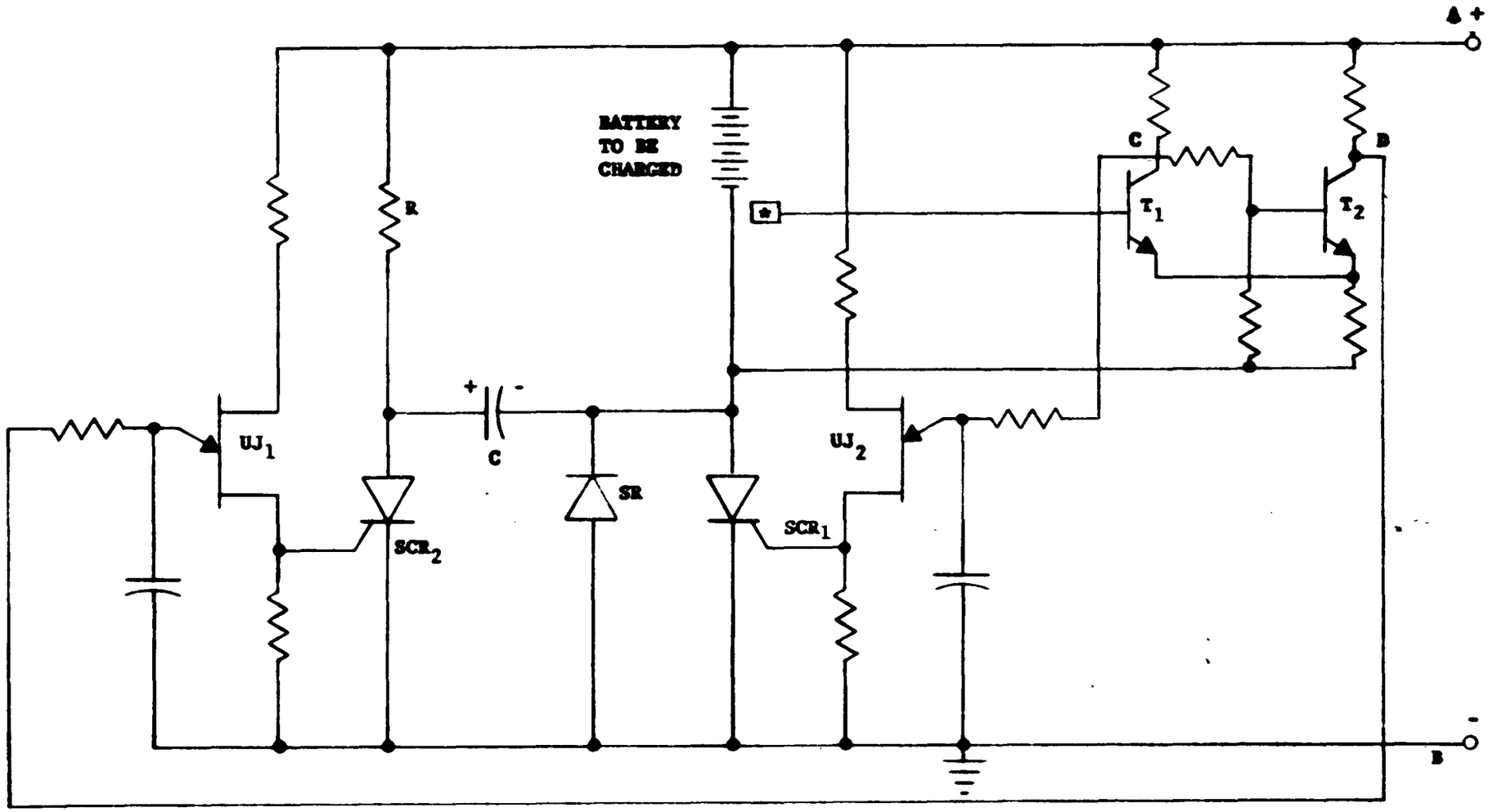

FIGURE 21 - CHARGE CONTROL CIRCUIT

* COULOMETER, AMPYBROOK, OR PRESSURE SWITCH

DISTRIBUTION LIST
WRIGHT-PATTERSON AIR FORCE BASE
AERONAUTICAL SYSTEMS DIVISION

CONTRACT NO. AF 33(615)2087
AB 8590

ACTIVITIES AT W.P.A.F.B.

ONE (1) COPY TO EACH OF THE FOLLOWING SYMBOLS

S.E.T.R.R. (1)
A.P.E. (1)

FOUR (4) COPIES TO:

Mr. R. A. Marsh (4)
APIP-2
Aeronautical Systems Division
Wright-Patterson Air Force Base, Ohio

OTHER DEFENSE DEPT. ACTIVITIES

Dr. Adolph Fishback (1)
Special Purposes Battery Branch
Power Sources Div.
U.S.A.S. Research & Development Labs.,
ATT: SIGRA/SL-PSS
Fort Monmouth, N. J.

OASD (RNE) (1)
Room RM 3E-1065
Pentagon
ATT: Technical Library
Washington, D. C.

Commanding Officer (1)
Diamond Ordinance Fuze Lab.
ATT: Library Room 211
Building 92
Washington 25, D. C.

USAS Research & Development Lab. (1)
ATT: Mr. Paul Rappaport
Fort Monmouth, New Jersey

Mr. E. F. Cogswell
Electrical Power Branch
Engineering Research & Development Lab. (1)
Ft. Belvoir, Va.

NAVY

Mr. P. Cole (1)
Naval Ordinance Laboratory
(Code WB)
Silver Springs, Maryland

A.F.C.R.L. (CRZK Mr. Dougherty) (1)
L. G. Hanscome Field
Bedford, Mass.

Mr. W. H. Fox (1)
Office of Naval Research
(Code 425)
Department of Navy
Washington 25, D. C.

Naval Ordinance Lab. (1)
ATT: W. C. Spindler
Corona, California

SSD (SSTRE MAJOR ILLER) (1)
Air Force Unit Post Office
Los Angeles 45, California

Defense Documentation Center (20)
Cameron Station
Alexandria, Virginia 22314

NASA (1)
ATT: Mr. Walter Scott
1512 "H" Street, N. W.
Washington 25, D. C.

NASA-Lewis Research Center (1)
ATT: Dr. Lewis Rosenblum
21,000 Brookpark Road
Cleveland 35, Ohio

NASA-Marshall Space Flight Center (1)
ATT: M-G and C-EC
Mr. E. H. Cagle
Building 4487 - Guid. and Control
Huntsville, Alabama

INDUSTRY

Aerospace Corporation (1)
P. O. Box 95085
Los Angeles 45, California

Jet Propulsion Laboratory (1)
California Institute of Technology
4800 Oak Park Drive
Pasadena, California

DISTRIBUTION LIST
WRIGHT-PATTERSON AIR FORCE BASE
AERONAUTICAL SYSTEMS DIVISION

CONTRACT NO. AF 33(615)2087
AB-8590

Delco Remy Division (1)
General Motors Corporation
ATT: Mr. J. J. Lander
Anderson, Indiana

Dr. T. P. Dirkse (1)
Dept. of Chemistry,
Calvin College
Grand Rapids, Michigan

Dr. Arthur Fleischer (1)
466 South Center Street
Orange, New Jersey

P. R. Mallory & Co., Inc. (1)
Laboratory for Physical Science
ATT: F. J. Cocca
N. W. Industrial Park
Burlington, Mass.

Inland Testing Laboratories (1)
Division of Cook Electric Co.
1482 Stanley Ave.
Dayton, Ohio

Lockheed Missiles & Space Co. (1)
ATT: Dr. J. E. Chilton
3251 Hanover Street
Palo Alto, California

Scientific & Technical Information Facility (2)
ATT: NASA Representative (SAK/DL)
P. O. Box 5700
Bethesda, Maryland 20014

Hq. FAA
ATT: Mr. D. G. Middlebrook (RD-221)
800 Independence Ave., S.W.
Washington, D. C. 20553